(12)

DNA-TR-85-324

SCALE EFFECTS ON THE BEHAVIOR OF SHALLOW-BURIED STRUCTURES, AND CRITERIA FOR SHOCK EFFECTS ON GROUND-SUPPORTED EQUIPMENT

J. D. Haltiwanger
W. J. Hall
H&H Consultants, Inc.
Room B106A, Newmark Laboratory
208 N. Romine Street
Urbana, IL 61801-2379

31 August 1985

Technical Report

CONTRACT No. DNA 001-84-C-0026

THIS WORK WAS SPONSORED BY THE DEFENSE NUCLEAR AGENCY
UNDER RDT&E RMSS CODE B344084466 Y99QMXSC00090 H2590D.

Prepared for
Director
DEFENSE NUCLEAR AGENCY
Washington, DC 20305-1000

DISTRIBUTION LIST UPDATE

This mailer is provided to enable DNA to maintain current distribution lists for reports. We would appreciate your providing the requested information.

☐ Add the individual listed to your distribution list.

☐ Delete the cited organization/individual

☐ Change of address.

NAME: _____

ORGANIZATION: _____

OLD ADDRESS	CURRENT ADDRESS
_____	_____
_____	_____
_____	_____

TELEPHONE NUMBER: ( ) _____

SUBJECT AREA(s) OF INTEREST:

_____ _____

_____ _____

_____ _____

DNA OR OTHER GOVERNMENT CONTRACT NUMBER: _____

CERTIFICATION OF NEED-TO-KNOW BY GOVERNMENT SPONSOR (if other than DNA):

SPONSORING ORGANIZATION: _____

CONTRACTING OFFICER OR REPRESENTATIVE: _____

SIGNATURE: _____

UNCLASSIFIED
SECURITY CLASSIFICATION OF THIS PAGE

REPORT DOCUMENTATION PAGE

Form Approved
OMB No. 0704-0188
Exp. Date: Jun 30, 1986

1a. REPORT SECURITY CLASSIFICATION UNCLASSIFIED	1b. RESTRICTIVE MARKINGS
2a. SECURITY CLASSIFICATION AUTHORITY N/A since Unclassified	3. DISTRIBUTION/AVAILABILITY OF REPORT Approved for public release; distribution is unlimited.
2b. DECLASSIFICATION/DOWNGRADING SCHEDULE N/A since Unclassified	
4. PERFORMING ORGANIZATION REPORT NUMBER(S)	5. MONITORING ORGANIZATION REPORT NUMBER(S) DNA-TR-85-324
6a. NAME OF PERFORMING ORGANIZATION H&H Consultants, Inc. 6b. OFFICE SYMBOL (If applicable)	7a. NAME OF MONITORING ORGANIZATION Director Defense Nuclear Agency
6c. ADDRESS (City, State, and ZIP Code) Room B106A, Newmark Laboratory 208 N. Romine Street Urbana, IL 61801-2379	7b. ADDRESS (City, State, and ZIP Code) Washington, DC 20305-1000
8a. NAME OF FUNDING/SPONSORING ORGANIZATION 8b. OFFICE SYMBOL (If applicable)	9. PROCUREMENT INSTRUMENT IDENTIFICATION NUMBER DNA 001-84-C-0026
8c. ADDRESS (City, State, and ZIP Code)	10. SOURCE OF FUNDING NUMBERS PROGRAM ELEMENT NO: 62715H; PROJECT NO: Y99QMXS; TASK NO: C; WORK UNIT ACCESSION NO: DH007923

11. TITLE (Include Security Classification)
SCALE EFFECTS ON THE BEHAVIOR OF SHALLOW-BURIED STRUCTURES, AND CRITERIA FOR SHOCK EFFECTS ON GROUND-SUPPORTED EQUIPMENT

12. PERSONAL AUTHOR(S)
Haltiwanger, J.D.; Hall, W.J.

13a. TYPE OF REPORT	13b. TIME COVERED	14. DATE OF REPORT (Year, Month, Day)	15. PAGE COUNT
Technical	FROM 831021 TO 850831	850831	90

16. SUPPLEMENTARY NOTATION
This work was sponsored by the Defense Nuclear Agency under RDT&E RMSS Code B344084466 Y99QMXSC00090 H2590D.

17 COSATI CODES		
FIELD	GROUP	SUB-GROUP
20	11	
11	2	

18. SUBJECT TERMS (Continue on reverse if necessary and identify by block number)
Shallow-Buried Structures; Shock Effects; Dynamic Response; Ground Shock; Scale Effects; Nuclear Blast Effects

19. ABSTRACT (Continue on reverse if necessary and identify by block number)

This report consists of two parts. In Section 1, the possible influences of scale (size of structure) on the response of shallow-buried reinforced concrete structures to nuclear-blast-induced surface overpressures are studied. It is concluded that such effects, if they exist at all, are negligible at scales equal to or greater than one-quarter. At very small scales, the evidence as to the significance of scale effects is inconclusive.

In Section 2, detailed consideration is given to the nature of the criteria that should be employed in the evaluation of shock effects on ground-supported equipment. Specific attention is given to the various types of ground-supported equipment that are of importance; the environmental factors that affect the shock loading and resistance characteristics of such equipment; the mounting motion and damage mechanisms of equipment items; and the methods of analysis, testing and design of equipment and its mountings. An effort

20. DISTRIBUTION/AVAILABILITY OF ABSTRACT ☐ UNCLASSIFIED/UNLIMITED ☒ SAME AS RPT ☐ DTIC USERS	21. ABSTRACT SECURITY CLASSIFICATION UNCLASSIFIED
22a. NAME OF RESPONSIBLE INDIVIDUAL Betty L. Fox	22b. TELEPHONE (Include Area Code) (202) 325-7042 22c. OFFICE SYMBOL DNA/STTI

DD FORM 1473, 84 MAR — 83 APR edition may be used until exhausted. All other editions are obsolete.

SECURITY CLASSIFICATION OF THIS PAGE
UNCLASSIFIED

18. SUBJECT TERMS (Continued)

Equipment Fragility

19. ABSTRACT (Continued)

is made to provide a comprehensive overview of the current state of the art for this very complex subject.

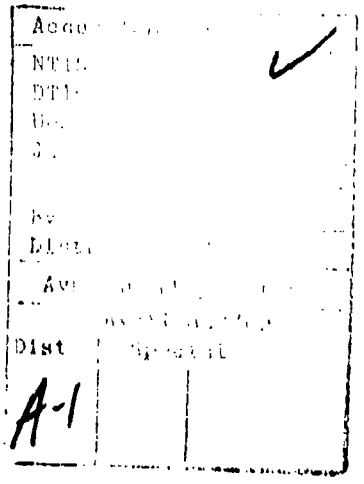

PREFACE

The work reported herein was sponsored by the Defense Nuclear Agency under Contract DNA 001-84-C-0026. The total contract effort consisted of the following four tasks.

Task 1: A study of the effects of the recently revised predictions of free-field pressure pulse shapes on the vulnerability radii of typical urban-industrial targets.

Task 2: Criteria considerations for shock effects on ground supported equipment.

Task 3: A review of the data collected during the shallow-buried structures test series in an effort to understand better the behavior and failure mechanisms of those structures.

Task 4: A series of special projects identified and assigned by the CTM during the course of the contract.

This report summarizes the work that was completed during the contract period on Task 2 and Task 3. An interim report covering the work completed under Task 1 was issued on 15 December 1984 and the work done under Task 4, which consisted primarily of participation on a number of DNA advisory groups, was reported to the appropriate agencies as it was accomplished.

Additional free-field data have been received recently which will permit the work reported earlier under Task 1 to be extended under a recently approved contract, DNA 001-C-85-0251. Similarly, additional work that was begun under Task 3 will also be extended and reported under this new contract.

The work reported herein was done by Drs. W. J. Hall and J. D. Haltiwanger, principals of H&H Consultants, Inc., who were assisted by Mr. James D. Buckler, a graduate student at the University of Illinois. Dr. Kent L. Goering served as the Contract Technical Monitor for the project.

CONVERSION TABLE

CONVERSION FACTORS FROM U.S. CUSTOMARY TO SI UNITS OF MEASUREMENT

To Convert From	To	Multiply By
foot	meter (m)	0.30480
Foot-pound-force	joule (J)	1.3558
inch	meter (m)	0.0254
kip (1000 lbf)	newton (N)	4448.2
kips/inch^2 (ksi)	kilo pascal (kPa)	6894.8
pound-force	newton (N)	4.4482
pound-force inch	newton-meter (N m)	0.11298
pound-force/inch	newton-meter (N/m)	175.13
pound-force/foot^2	kilo pascal (kPa)	0.04788
pound-force/inch^2	kilo pascal (kPa)	6.8947
pound-mass	kilogram (kg)	0.45359

TABLE OF CONTENTS

LIST OF ILLUSTRATIONS

LIST OF TABLES

SECTION 1

AN INVESTIGATION OF POSSIBLE SCALE EFFECTS ON THE DYNAMIC RESPONSE OF SHALLOW-BURIED REINFORCED CONCRETE STRUCTURES

1.1 BACKGROUND.

In the late 1970's, recognizing that the procedures that were then being used to estimate the vulnerability levels of shallow buried structures were largely unsupported by experimental evidence, the Defense Nuclear Agency inaugurated a program that was designed to overcome this deficiency. This program, which came to be known as the Shallow-Buried-Structures or SBS Research Program, was carried out over approximately six years and had as its primary thrust the testing by the U.S. Army Waterways Experiment Station of a series of quarter-scale models of simply configured shallow buried structures. Reports of these tests are contained in References 1 through 6.

The culmination of this program was the publication in 1984 of a report entitled "Vulnerability of Shallow-Buried Flat-Roof Structures, Final Report: A Computational Procedure", by Kiger, Slawson, and Hyde (Ref. 7). This 1984 report which was written against a background of the accumulated experimental evidence, provided a new procedure for estimating the vulnerability of shallow-buried, flat-roofed structures. The test results had demonstrated clearly that the previously-used predictive procedures had grossly underestimated the vulnerability levels of such structures and the revised procedures, which were promulgated in the 1984 report, corrected this deficiency.

But it was then observed that the test data on which the newly developed predictive procedures were based had all been obtained from tests of quarter-scale models, leaving open the possibility that those results might have been biased as a consequence of scale effects. To investigate this possibility, at least to a limited extent, a half-scale model of the same structure that had been tested in quarter-scale in several of the earlier experiments was tested in FY 1985. Additionally, the results that had been obtained in tests of a twelfth-scale model of the same structure in the Mighty-Mach series in Canada in 1979 were also introduced into the study.

This report contains a summary of studies that were made of the several data sources noted above in an effort to assess the extent, if any, to which the results of the quarter-scale SBS tests, which had provided the basis for the proposed revision of the vulnerability analysis procedures, may have been called into question by scale effects.

1.2 OBJECTIVES AND SCOPE OF STUDY.

As noted above, the objective of this effort was to study the available pertinent data and assess the extent to which the data that had been taken in the quarter-scale SBS test series might have been compromised as a consequence of scale effects that were inherent in the model tests. To this end, attention was directed to the results that had been obtained in a set of experiments which were very similar, one to another, except for the scales at which the tests were conducted.

The tests that were considered in this study are listed below, and are very briefly described. More complete descriptions of these tests are contained in a subsequent section of this report.

(1) Foam HEST 4: A quarter-scale model of a single-bay reinforced concrete box as illustrated in Fig. 1, with a clear roof span of 4.0 ft, and a internal length of 16 ft.

(2) Foam HEST 7: A quarter-scale model of a three-bay reinforced concrete box similar to the Foam HEST 4 box, but having three adjacent continuous cells, as shown in Fig. 1(c), each of which has a clear span of 4.0 ft.

(3) Dynamic Shear Test No. 3: A quarter-scale model of a single-bay reinforced concrete box, which had the same cross-section as did the box of the Foam HEST 4 test, but which was cast without endwalls, was only 4.0 ft. long, and was tested in a set-up that was designed to insure one-way roof slab behavior. In contrast, the roofs of the Foam HEST 4 and 7

test structures were two-way slabs having aspect ratios of 1/4.

(4) FY-85 Half-Scale Test: A test that was identical to that of Foam HEST 4 except that the structure was at half-scale and had, therefore, a clear short span of 8 ft.

(5) Mighty-Mach: A series of five similar tests of a structure as illustrated in Fig. 1 that was constructed at twelfth-scale. Its clear roof span was, therefore, only 16 inches, in comparison with the 48-inch clear spans of quarter-scale models noted above. Of the five tests that were run in this series, only two (Nos. 1 and 4) are directly comparable to the previously cited quarter- and half-scale tests. The other three tests (nos. 2, 3, and 5) differed either in their L/d ratios or in their depths of burial.

With the exception of Tests No. 2, 3, and 5 of the Mighty-Mach series, these experiments were all tests of rectangular, reinforced concrete box-type structures, all of which had roof clear-span-to-effective-depth ratios, L/d, of 10, were buried in sand to a depth of cover equal to L/5, were reinforced similarly with principal steel ratios of 0.01 on each face, and were loaded with air blast pressure pulses applied to the surface of the ground directly above the model structures. They were, therefore, almost identical, or at least closely comparable structures, except for the very substantial differences in scales that were employed.

It seemed reasonable, then, that the presence of significant scale effects might be detected by studying the extent to which the vulnerability analysis procedure that had been developed from the quarter-scale model test data could be used also to predict the behavior of similar structures of substantially different scales. Since that analysis procedure (Ref. 7) was developed directly from the quarter-scale data of the SBS research program, it certainly should

predict quite closely the maximum responses of the quarter-scale structures listed above (Foam HEST 4, Foam HEST 7, and Dynamic Shear Test No. 3). And, if scale effects are of little or no consequence, that analytical procedure should also predict closely the maximum responses of the half-scale and twelfth-scale models. Conversely, if scale effects are quite pronounced, one would not expect an analytical procedure to be applicable at scales that differed significantly from the scale of the structures whose test data provided the basis for its formulation. With this in mind, all of the structures that were tested in the cited experiments were analyzed using the procedure of Ref. 7, and the results of those predictive analyses were compared with the observed maximum responses.

1.3 DESCRIPTIONS OF TEST STRUCTURES.

Because detailed descriptions of the test structures that were considered in this study and of the experimental setups in which they were tested are contained in readily available sources that are referenced herein, those detailed descriptions will not be repeated here. However, for convenient reference, and to portray clearly both the similarities and the differences that existed among these several structures, the critical and distinguishing aspects of those structures are summarized briefly below.

1.3.1 Foam HEST 4.

Data Source: Ref. 2
Type of Structure: Single-bay, rectangular, reinforced concrete box of the type shown in Figs. 1(a) and (b).
Dimensions:
Clear transverse span, L = 4'0"
Clear longitudinal span, 4L = 16'0"
Clear internal height, H = L = 4'0"
Depth of Burial, DOB = L/5 = 9.6"
Thickness of roof, base, and walls, t = 5.6"
Effective depth of roof, base, and walls, d = 4.8"
Ratio of roof clear span to effective depth, L/d = 10
Principal reinforcement ratios, $\rho = \rho' = 0.01$
Material Properties:

Concrete compressive strength, f'_c = 6,700 psi
Steel tensile yield stress, f_y = 65,000 psi

1.3.2 Foam HEST 7.

Data Source: Ref. 5
Type of Structure: Three-bay, rectangular reinforced concrete box of the type shown in Figs. 1(a) and (c).
Dimensions:
Clear transverse span, L = 4'0" for each bay
Clear longitudinal span, 4L = 16'0" for each bay
Clear internal height, H = L = 4'0" for each bay
Depth of Burial, DOB = L/5 = 9.6"
Thickness of roof, base, and external walls, t = 5.6"
Thickness of internal walls, t = 4.0"
Effective depths of roof, base, and external walls, d = 4.8"
Ratio of roof clear span to effective depth, L/d = 10
Principal reinforcement ratios, $\rho = \rho' = 0.01$
Material Properties:
Concrete compressive strength, f'_c = 5,100 psi
Steel tensile yield stress, f_y = 71,000 psi

1.3.3 Dynamic Shear Test No. 3.

Data Source: Ref. 6
Type of Structure: A single-bay, rectangular reinforced concrete box identical to that of Foam HEST 4, except that it is only 4.0 ft. long and has no endwalls.
Dimensions: Identical to those of Foam HEST 4, except as noted above.
Material Properties:
Concrete compressive strength, f'_c = 4,040 psi
Steel tensile yield stress, f_y = 62,750 psi

1.3.4 FY-85 Half-Scale Test.

Data Source: Ref. 8
Type of Structure: A single-bay, rectangular, reinforced concrete box of the type illustrated in Figs. 1(a) and (b). It differs from the structure of Foam HEST 4 only in that, at half-scale, it is twice as big as is Foam HEST 4, which is at quarter-scale.
Dimensions:
Clear transverse span, L = 8'0"
Clear longitudinal span, 4L = 32'0"
Clear internal height, H = L = 8'0"
Depth of Burial, DOB = L/5 = 19.2"
Thickness of roof, base, and walls, t = 11.2"
Effective depths of roof, base, and walls, d = 9.6"
Ratio of roof clear span to effective depth, L/d = 10

Principal reinforcement ratios, $\rho = \rho' = 0.01$

Material Properties:

Concrete compressive strength, $f'_c = 7{,}000$ psi

Steel tensile stress, $f_y = 66{,}000$ psi

1.3.5 Mighty-Mach Tests 1 and 4.

Data Source: Ref. 9

Type of Structure: A single-bay, rectangular, reinforced concrete box of the type illustrated in Figs. 1(a) and (b). It differs from the structure of Foam HEST 4 only in that, at twelfth scale, it is one-third as large as is the Foam HEST 4 structure.

Dimensions:

Clear transverse span, L = 1'4" = 16"

Clear longitudinal span, 4L = 5'4" = 64"

Clear internal height, H = L = 1'4" = 16"

Depth of Burial, DOB = L/5 = 3.2"

Thickness of roof, base, and walls, t = 2.4"

Effective depths of roof, base, and walls, d = 1.6"

Ratio of roof clear span to effective depth, L/d = 10

Principal reinforcement ratios, $\rho = \rho' = 0.01$

Material Properties:

Concrete compressive strength, $f'_c = 6{,}000$ psi

Steel tensile yield stress, $f_y = 60{,}000$ psi

1.4 DESCRIPTION OF ANALYTICAL PROCEDURE.

Each of the structures that was described in the preceding section was subjected, in an experiment bearing the same name as that given herein to the structure, to the effects of an air blast pressure loading on the surface of the ground above the structure. Consistent with the objectives of this study, the response of each of those structures to the applied air blast pressures was predicted using the computational method that is described in Ref. 7. As previously observed, that method was developed through the SBS Research Program by Kiger, Slawson, and Hyde, and was published in September 1984 by the U.S. Army Waterways Experiment Station as "Technical Report SL-80-7, VULNERABILITY OF SHALLOW-BURIED FLAT-ROOF STRUCTURES, Report 6, Final Report: A Computational Procedure".

For a complete description of that computational method, the reader is referred to Ref. 7. However, for convenient reference, and to facilitate discussion of the results obtained in this study, a

summary of that computational procedure is given in the paragraphs that follow.

The soil-structure system that is to be analyzed was modelled as a single-degree-of-freedom system whose loading and resistance functions are of the forms illustrated in Figs. 2 and 3, respectively. Brief descriptions of each of those functions are given below.

1.4.1 The Loading Function.

The loading function is characterized by an initially peaked but rapidly decaying spike of pressure which is followed by a more gradually decaying pulse that is defined by the function $C_a P_z(t)$. The initial peak pressure is equal to the reflected value of the attenuated peak surface overpressure at a depth equal to the depth to the roof of the structure being tested, and is given by

$$B = R\alpha_z P_{so} \tag{1}$$

where:

R = reflection factor (taken as 1.6 in these studies)

α_z = attenuation factor at depth z = DOB, which is a function of the peak surface overpressure, the weapon yield, the depth z, and the soil type as represented by its strain recovery ratio. For the sands used in these tests, the strain recovery ratio, r, was taken to be 0.1, in which case the attenuation factor is given by Fig. 2.1 of Ref. 7, which is reproduced herein as Fig. 4.

P_{so} = peak surface overpressure

The duration of that initial reflected spike T_B, is given by

$$T_B = \frac{12t}{c} \quad \text{or} \quad \frac{(\sqrt{r} + 1)\ (DOB)}{C_L}, \quad \text{whichever is smaller,} \tag{2}$$

where:

t = roof thickness, in ft.

c = seismic velocity in the roof (taken as 10,000 fps for the concrete in these structures)

r = strain recovery ratio for the backfill material (taken as 0.1 for the sand used in these experiments)

C_L = loading wave velocity in the backfill (taken as 1500 fps in these tests)

DOB = depth of burial to roof of structure, in ft.

The loading function that continues beyond the initial spike of reflected pressure is equal simply to the free-field vertical soil pressure at depth z = DOB, $p_z(t)$, multiplied by a soil arching factor, C_a. The free-field vertical soil stress at depth z = DOB is defined somewhat arbitrarily, but in a manner that conserves the surface impulse. It is taken as the Brode surface burst pressure-time history for which the initial peak value, P_{zo}, is equal to the attenuated peak pressure, $\alpha_z p_{so}$, and whose subsequent decay is described by a weapon yield, W_z, which was selected so that at a peak overpressure of p_{zo} it would generate a total overpressure positive phase impulse that is equal to the positive phase impulse that was contained under the actual surface pressure pulse. Detailed procedures for this computation are contained in Ref. 7.

The arching factor, C_a, is computed as a function of the plan dimensions of the structure, the depth of cover over the structure, and the properties of the soil backfill, from

$$C_a = \exp\left[-\frac{2K_o(\tan\phi_f)(L_S + L_L)(DOB)}{L_S L_L}\right] \qquad (3)$$

where:

K_o = coefficient of lateral earth pressure (assumed, for the sands used in these tests, to vary from about 0.3 to 0.5)

ϕ_f = angle of shearing resistance at depth of DOB (Assuming a basic angle of internal friction of about 35 degrees, computed for these tests to be about 38.5 degrees)

L_S = short span of roof, in feet

L_L = long span of roof, in feet

1.4.2 The Resistance Function.

The resistance function proposed for use in SDOF model of Ref. 7 is as illustrated in Fig. 3. Because Ref. 7 is readily available, the reproduction here of the relatively cumbersome procedures and equations

that are required to evaluate the various quantities needed to define the resistance function for a particular structure seems unnecessary. Hence, for those computational details, the reader is referred to that source. However, the following general description of the resistance function may be helpful at this point.

It consists of an initial elastic slope defined by a stiffness, K, up to a maximum resistance of r_u, which is computed as the ultimate flexural resistance of the roof slab, taking into account the resistance augmenting effects of both the in-plane forces that are generated in the slab by the engulfing blast-induced pressure in the soil and of the dynamic strain rate effects on the material properties.

After reaching a maximum value of r_u, the resistance stays constant at that level until it reaches a deflection of $2y_e$, where y_e is the initial elastic yield deflection.

Beyond a deflection of $2y_e$, the resistance decays on a slope of K_1, during which phase the augmenting effects of the in-plane forces are dissipated. This decay phase continues until the resistance becomes equal to r_o, the flexural resistance of the roof slab without the beneficial effects of in-plane forces, or until it intersects the final phase which is defined by a straight line of slope K_2 which passes through the origin, whichever occurs first. If the latter condition controls, the deflection ordinates identified on Fig. 3 as y_{p2} and y_t will merge into one point, the resistance value for which will be greater than r_o.

The final phase of the resistance function, which is defined by a slope of K_2, represents the resistance of the roof structure after it has been transformed, as a consequence of deformation, from a slab into a tensile membrane, for which the strength is derived entirely from the tensile capacities of the reinforcing steel in the slab.

1.4.3 The Natural Period of Vibration.

The natural period of vibration of the roof slab was computed from the following approximate but acceptable equations.

$$\frac{1}{T_2} = \frac{1}{T_{1L}} + \frac{1}{T_{1s}} \qquad (4)$$

and

$$T_1 = \frac{L^2}{5900d\sqrt{\rho}} \tag{5}$$

where:

T_2 = period of a two-way slab (sec)

T_1 = period of a one-way slab (sec), and the S and L subscripts refer to the short and long span directions of the roof slab

L = span of the slab (ft)

d = effective depth of the slab (in.)

ρ = tensile steel reinforcement ratio

1.4.4 The Response Computation Procedure.

The resistance functions of the structures of interest having been defined as described above, their responses to the imposed dynamic loading pulses were then computed as for undamped single-degree-of-freedom systems. Such responses are given by

$$M\ddot{Y}_y + R_y = F(t) \tag{6}$$

in which M = effective mass

$\ddot{Y}_t$ = acceleration at time, t

R_y = resistance at deflection, y

and, F(t) = blast-induced force applied to the structure at time t, determined as described earlier in this section.

The effective mass, M, for each structure studied was computed from

$$M = KT^2/4\pi^2 \tag{7}$$

in which K and T are, respectively, the initial elastic slope of the resistance function and the natural period of vibration of the structure.

This equation of motion was solved by the "Modified Beta Method" of step-by-step integration, which is a modification of Newmark's "Beta Method" (see Ref. 10). Using this method, and assuming the acceleration, velocity, and displacement of the mass to be known at time t, the velocity and displacement of the mass at the end of a time increment of duration h are given by

$$\dot{Y}_{t+h} = \dot{Y}_t + \frac{h}{2}(\ddot{Y}_t + \ddot{Y}_{t+h}) \tag{8}$$

and

$$Y_{t+h} = Y_t + h\dot{Y} + (1/2 - \beta)\, h^2\ddot{Y}_t + \beta h^2\ddot{Y}_{t+h} \tag{9}$$

in which Y_t = displacement at beginning of time interval

$\dot{Y}_t$ = velocity at beginning of interval

$\ddot{Y}_t$ = acceleration at beginning of interval

Y_{t+h} = displacement at end of interval

$\dot{Y}_{t+h}$ = velocity at end of interval

$\ddot{Y}_{t+h}$ = acceleration at end of interval

h = length of time interval

β = a constant whose value defines the variation in acceleration during the time interval h (selected as 1/6 for this study)

If the resistance, R, at time t+h, is defined in terms of the resistance function parameters and the deflection, Y_{t+h}, and Eqs. (8) and (9) are substituted into Eq. (6), a direct solution of Eq. (6) for $\ddot{Y}_{t+h}$ yields

$$\ddot{Y}_{t+h} = \frac{F_{t+h} + K[D - Y_t - h\dot{Y}_t - (\frac{1}{2} - \beta)\, h^2\ddot{Y}_t] - Z}{M + K\beta h^2} \tag{10}$$

in which F_{t+h} = applied force at time t+h

h = length of time interval

K = slope of the resistance function in the domain of the deflection that occurs during the time interval, h

D = deflection which defines the beginning of the straight-line segment of the resistance function of slope, K, along which motion occurs during the time interval, h

Z = resistance corresponding to the deflection D

M = mass of the responding system

and the other terms of Eq. (10) are as previously defined.

Hence, by solving Eqs. (10), (8), and (9) successively and repetitively at time increments of h, the maximum deflection of the structure to any applied blast-induced loading can be computed.

As noted above, β was selected to have a value of 1/6 for this study. This value corresponds to a linear variation in the acceleration, $\ddot{Y}$, during the time interval, h, used in each integration step. Assuming that suitably small values of h are used, such a variation of acceleration during the time interval should be an acceptable approximation of the real variation.

Clearly, the precision of the results obtained by this procedure is influenced by the size of the time-interval, h, that is selected for use in the analyses. For this study, values of h were selected to be no greater than one-tenth of the natural period of vibration of the structure and, for time domains in which the pressure varied rapidly with time, much smaller time increments were used in order to represent the loading functions accurately.

The detailed calculations were carried out on an IBM Personal Computer using a program written in BASIC that was developed for this purpose.

1.5 RESULTS OF ANALYSES.

The responses of the six structures that were described in Section 1.3 to the air blast pressures under which they were tested were computed using the computational procedure that is summarized in Section 1.4 with the intention of comparing those computed results with the responses of those structures as observed in the actual tests.

In the sections that follow, for each of the test structures, the air blast pressure loading on the ground surface immediately above it

is briefly described. Then the SDOF loading and resistance functions that were developed for the roof slab, as outlined in Sections 1.4.1 and 1.4.2, are presented and the maximum deflection of the structure is then computed, using the analytical method that is described in Section 1.4.4. The detailed calculations that led to the loading and resistance functions are not shown, but to facilitate checking of those functions, intermediate parameters are defined which, while incidental to the calculations, are also particularly significant to them.

Regrettably, the basic input data that were required for the determination of the loading and resistance functions were sometimes not clearly defined in the data sources, necessitating in such instances, the use of assumed or estimated data. In those cases, a few additional analyses, over and above the first or basic analysis were run in which the parameters most affected by input data uncertainties were varied in modest amounts. Such additional runs were intended to provide at least a crude measure of the extent to which small variations in some of the more uncertain input data quantities would influence the validity of the computations.

1.5.1 Analysis of Foam HEST 4.

Surface Loading: An overpressure pulse that was generated by a Foam HEST test and reported in Ref. 2 as having reasonably simulated an overpressure pulse having a peak value of 1900 psi from a nuclear weapon having a yield of 0.85 KT, which was donated on the ground surface.

Roof Loading: A pulse, as shown in Fig. 5(a), of the general form illustrated by Fig. 2, for which the quantities shown thereon were computed as described in Section 1.4.1 from the ground surface loading defined immediately above. Significant to that computation was the determination of a soil arching factor, C_a, of 0.85, and of a pressure attenuation factor, α_z, for the ground surface loading pulse, of 0.80. The latter influences the values of both the peak initial reflected pressure on the roof and the vertical free-field pressure at the depth of the roof, which when multiplied by the soil arching factor, becomes the continuing component of the loading on the roof.

Resistance Function: As shown in Fig. 5(b), a function of the general form depicted in Fig. 3, computed on the basis of the structural dimensions and material properties as given in Section 1.3.1. In use, the static material strengths were increased by 30 percent in an effort to account for the dynamic strain rate effects. Incidental to the determination of this resistance function were also an assumed lateral soil pressure coefficient, K_o, of 0.5 and a pressure attenuation factor to mid-height of the wall of the structure, α_c, equal also to about 0.5.

For simplicity, although the roof was actually a two-way slab, its resistance was computed as for a one-way slab spanning in short dimension. This simplification seemed to be justified by the 1-to-4 aspect ratio of the slab and by the fact that the two-way effect was further minimized because only about half as much reinforcement was used in the long direction as was used in the short direction. Furthermore, the reinforcement in the long direction was placed at a smaller effective depth than was used in the short direction.

The Natural Period of Vibration was computed as outlined in Section 1.4.3 to be approximately 5.3 ms.

Results: For the basic system just described, the maximum deflection was computed to be 15.2 inches, which agrees quite well with the observed "near collapse" deflection of about 12.5 inches.

Because of uncertainties in the validity of some of the data that were used to generate the loading and resistance functions that were used for the basic analysis reported above, several parametric variation studies were also made, with the following results:

(a) If the soil arching factor, C_a, is taken to be 0.80 instead of 0.85, the maximum deflection is computed to be 14.2 inches.

(b) If the pressure attenuation factor, α_z, that is associated with the ground surface pressure pulse, is taken as 0.7 instead of 0.8, the resulting change in the roof loading function is such as to produce a maximum computed deflection of 13.9 inches.

(c) If a natural period of 5.8 ms is used instead of 5.3 ms, the maximum deflection is computed to be 14.1 inches.

1.5.2 Analysis of Foam HEST 7.

Surface Loading: An overpressure pulse generated by a Foam HEST test, and reported in Ref. 5 as reasonably simulating an overpressure pulse having a peak value of 2360 psi from a weapon of 1.2 KT yield detonated at zero-HOB.

Roof Loading: The pulse as shown in Fig. 6(a). Significant to the determination of that function was the intermediate evaluation of the pressure attenuation factor, α_z, and the soil arching factor, C_a, to be 0.8 and 0.85, respectively.

Resistance Function: The function as plotted in Fig. 6(b) computed on the basis of the structural dimensions and material properties as given in Section 1.3.2, and the following additional significant parameters:

Concrete and steel strain rate amplification factor = 1.3

Lateral soil pressure coefficient, K_o = 0.5

Pressure attenuation factor, α_o, to mid-depth of wall = 0.5

As for the previous case, for simplicity, the resistance was computed as for a one-way slab of the short span dimension.

The Natural Period was computed to be 5.3 ms, the same as it was found to be for Foam HEST 4.

Results: The computed maximum deflection was 18.5 inches, which would not be considered to be in disagreement with the results of the experiment in which the roof suffered complete collapse. Clearly, a deflection of 18.5 inches in a span of only 48 inches is sufficient to assume that collapse has either occurred or, at the least, is imminent.

No parameter variation analyses were made for this case.

1.5.3 Analysis of Dynamic Shear Test. No. 3.

Surface Loading: An overpressure pulse generated by a Foam HEST test and reported in Ref. 6 as reasonably simulating an overpressure pulse having a peak value of 3330 psi from a weapon of 0.23 KT yield detonated at zero-HOB.

Roof Loading: The pulse as shown in Fig. 7(a). In the development of that pulse, the pressure attenuation factor, α_z, was found to be approximately 0.6, and the soil arching factor was computed to be about 0.78. This arching factor was smaller than the value of 0.85 that was used in the other cases because, in this present case, the test setup was such that soil arching developed over a 4 by 4 ft plan area, instead of over the 4 by 16 ft plan area of the two prior cases.

Resistance Function: The function as plotted in Fig. 7(b), computed on the basis of the structural dimensions and material properties as given in Section 1.3.3, and the following additional significant parameters:

Concrete and steel strain rate amplification factor = 1.3

Lateral soil pressure coefficient, K_o = 0.5

Pressure attenuation factor, α_c, to mid-depth of wall = 0.34

This structure was a pure one-way slab, and the resistance was so computed.

As a one-way slab, the Natural Period was computed to be about 5.6 ms.

Results: The maximum deflection for the basic structure whose loading and resistance functions are as just described was computed to be 15.2 inches, which should be compared with the observed test deflections which varied from about 9.5 to 11 inches along the center-line of the slab.

Because of uncertainties in the input data, several parameter variation studies were also run, producing the results that are summarized below:

(a) If the soil arching factor is taken as 0.71 instead of 0.78 as estimated above, the maximum deflection is computed to be 14.0 inches.

(b) If the natural period of vibration is taken to be 6.6 ms instead of 5.6 ms, the computed maximum deflection is found to be 13.1 inches.

(c) If the period is taken as 6.6 ms and a soil arching factor of

0.71 is used, the maximum deflection is computed to be 12.0 inches.

1.5.4 Analysis of FY-85 Half-Scale Test.

Surface Loading: An overpressure pulse generated by a Foam HEST test, and reported in Ref. 8 as reasonably simulating an overpressure pulse having a peak value of 1284 psi from a weapon of 89.8 KT yield, detonated at zero-HOB.

Roof Loading: The pulse as shown in Fig. 8(a), significant to which were a soil arching factor evaluated to be 0.85 and a pressure attenuation factor which was also found to be 0.85.

Resistance Function: The function as plotted in Fig. 8(b), computed on the basis of structural dimensions and material properties as given in Section 1.3.4, and the following additional significant parameters:

Concrete and steel strain rate amplification factor = 1.3

Lateral soil pressure coefficient, K_o = 0.5

Pressure attenuation factor, α_o, to mid-depth of wall = 0.55

Consistent with the previously established practice, the resistance was computed as for a one-way slab.

The Natural Period was computed in the usual manner to be 10.8 ms.

Results: The maximum deflection of this structure was computed to be 36.4 inches, while a maximum deflection of about 50 inches was observed in the test. However, it should be noted that approximately six inches of the observed 50-inch maximum deflection resulted from very large inward motions of the tops of the side walls of the structure. Consequently, since the computational procedure takes no account of this latter effect, the computed deflections should be compared with an observed deflection of about 44 inches.

The effects of small variations in several of the significant parameters were studied, with the following results:

(a) If the pressure attenuation factor is taken as 0.9 instead of 0.85, the roof loading function is changed and the maximum deflection is computed to be 37.8 inches.

(b) If a soil arching factor of 0.9 instead of 0.85 is used, the computed maximum deflection is 38.9 inches.

(c) If the period is changed from 10.8 ms to 11.8 ms, the computed maximum deflection is reduced to 34.6 inches.

(d) If a period of 9.8 ms is used instead of 10.8 ms, the computed deflection becomes 38.4 inches.

(e) If the resistance-augmenting effects of in-plane forces are non-existent (or neglected), the resistance would become an elasto-plastic function with the same initial stiffness as before (See Fig. 8(b)), but with a yield resistance of only 129 psi, which is followed, at deflections greater than 8.66 inches, by the tension membrane phase as shown in Fig. 8(b). For such a resistance, with no other changes, the maximum deflection is computed to be 39.6 inches.

1.5.5 Analysis of Mighty Mach Test No. 1.

Surface Loading: In contrast to the other cases which were Foam HEST tests, this model was loaded by the detonation of an 1100 pound sphere of pentolite at an HOB of 15 feet, while the model was located at a horizontal ground range of 3.79 ft. The data report, Ref. 9, recommends that the blast pressure on the ground surface directly above the model structure be estimated as the average of the two pressure records that are reproduced herein as Fig. 9.

To obtain such an "average" curve, each of those two curves was read by eye at the same time increments, producing the pressure-time data that are contained in Tables 1 and 2. It should be observed in those tabulations that the accumulated impulses associated with the tabulated pressure-time pairs agree very closely with the corresponding accumulated impulses as read from the original data curves in Fig. 9. The surface loading for this test was then computed as the average of the curves represented by the data of Tables 1 and 2, which is tabulated in Table 3 and is plotted in Fig. 11.

No nuclear weapon overpressure pulse could be identified for which the average pressure curve just developed was a reasonable simulation. The total impulse under it is reasonably well represented in both

magnitude and time-wise distribution by the overpressure pulse produced at a ground range of 3.79 ft. from a weapon of 0.0013 KT yield exploded at an HOB of 15.0'. But, as is evident in the parallel tabulations of Table 3, both the peak pressure and the initial decay slope of the latter are much greater than they are for the averaged pulse.

Similarly, the initial peak pressure and the pulse shape for about the first half-millisecond are reasonably replicated by the overpressure pulse produced at a range of 51.3 ft by the detonation of a 0.1 KT weapon at zero-HOB. But both the duration of this pulse and the total impulse contained in it are much larger than are the comparable quantities of the "average" pulse.

Roof Loading: As for the other cases treated thus far, the roof loading should be of the general form shown in Fig. 2, and should be derived from the ground surface pressure loading in the manner described in Ref. 7. But since the ground surface pressure function is not reasonably represented by a "simulated" surface burst nuclear pulse, this cannot be accomplished in the prescribed manner. Specifically, neither the pressure attenuation factors nor the free-field vertical pressure pulse at depth can be determined with confidence.

In the absence of a better procedure, it was assumed that the pressure attenuation factor, α_z, was influenced primarily by the initial peak pressure and the shape of the surface pulse in its very early time history. On the basis of this assumption, a ground surface overpressure pulse having a peak value of 2700 psi from a 0.1 KT weapon led to an attenuation factor of approximately 0.8. Then, consistent with the idea that the surface impulse should be preserved at the depth of the roof, the free-field pulse at that depth was computed from the ground surface pulse as tabulated in Table 3 and plotted in Fig. 11 by multiplying those pressure ordinates by the attenuation factor and dividing the time scale by that same factor, 0.8 in this case.

Having thus defined the attenuation factor, and the free-field vertical soil stress pulse at the depth of the roof, the roof loading was generated in the normal fashion and is as shown in Fig. 12(a).

Resistance Function: The function as plotted in Fig. 12(b), computed on the basis of the structural dimensions and material properties as given in Section 1.3.5, and the following additional significant parameters:

Concrete and steel strain rate amplification factor = 1.3

Lateral soil pressure coefficient, K_o = 0.5

Pressure attenuation factor, α_o, to mid-depth of wall = 0.5

For reasons given in cases previously treated, the two-way aspects of the roof were neglected, and the resistance function was determined as for a one-way slab whose span was the short dimension of the roof. As for the roof load determination, it was assumed here that the pressure attenuation factor to mid-height of the wall could be estimated on the assumption that the surface pulse was that of a 0.1 KT surface burst.

The Natural Period was estimated in the usual manner and found to be 1.77 ms.

Results: The maximum deflection for the model just described was computed to be 4.6 inches, which is to be compared with a measured maximum deflection in the first Mighty Mach experiment of only 1.75 inches. It should be observed, however, that this quite substantial difference in observed and computed deflections may be explained, at least in part, by the manner in which the pressure attenuation factors were estimated. Determined as it was, it almost certainly represented an upper bound on the value of the attenuation factor, with the result that the roof loading was somewhat greater than it should have been and the computed deflection was, correspondingly, too high.

To gain some insight in the significance of this problem, consideration was given to what might be called the other extreme. The problem was re-analyzed on the assumption that the ground surface loading was reasonably defined by the overpressure pulse produced at a range of 3.79 ft. by a weapon of 0.0013 KT yield detonated at an HOB of 15 ft. As noted earlier, such a pulse (see Table 3) matches quite well the desired impulse of the surface loading pulse, but departs very substantially from the desired wave form.

If that 0.0013 KT pulse is used as a basis, the attenuation factor at roof depth is estimated to be about 0.4 and a roof loading function

as shown in Fig. 13(a) is produced. (At this point, it should be noted, following the procedures of Ref. 7, that the attenuation factor was determined on the assumption that the surface pressure function was produced by a surface burst. Since the pulse used was from an above-ground burst, the initial pressure decay rate is somewhat less than its surface-burst counter-part would have exhibited. As a consequence, the attenuation factor of 0.4 is probably slightly smaller than it should be.)

In like manner, a revised resistance function corresponding the new (different?) surface loading was developed and is as shown in Fig. 13(b).

A response analysis of this structure, with the newly defined surface loading on it, produced a maximum computed response of 4.2 inches, which is only 0.2 inches less than previous analysis gave.

1.5.6 Analysis of Mighty Mach Test No. 4.

Surface Loading: The loading for this test differed from that of Mighty Mach Test No. 1 only in that the 1100-pound pentolite sphere was detonated at an HOB of 10 ft instead of 15 ft. As in the previous case, the data source (Ref. 9) recommends that the ground surface loading directly above the model structure be approximated as the average of two pressure gage records. Those two records are reproduced herein as Fig. 10(a) and (b).

The average of those two pressure records was developed in the same way that the corresponding "average" pressure loading on the ground surface for the previous case was developed. Tables 4 and 5 are tabulations of the pressures read from the curves of Fig. 10 and Table 6 contains a listing of the averages of the data in Tables 4 and 5. For ease of comparison with the surface pressure pulse that was developed for Mighty Mach Test No. 1, the pulse represented by the data of Table 6 is also plotted in Fig. 11.

As was the situation in the first Mighty Mach test, the ground surface loading pulse shown in Fig. 11 is not a reasonable simulation of any single nuclear weapon overpressure curve. Its peak pressure and its very early time shape are quite closely duplicated by the

overpressure pulse of the same peak value that is produced at a range of 90 ft by a surface burst weapon of 1.0 KT yield. But the impulse under the curve is reasonably well approximated (especially for times greater than 0.5 ms) by the overpressure pulse generated at a ground range of 3.79 ft by a 0.009 KT weapon detonated at an HOB of 10 ft, which are the HOB and range of the actual test. It should be observed, as is evident from the data of Table 6, that this impulse-equivalent pulse has a much higher initial peak value as well as a much steeper initial decay rate than does the pulse being approximated.

Roof Loading: The roof loading function for this case was developed in the same way in which the loading function for the Mighty Mach Test No. 1 case was developed.

Assuming that the pressure attenuation factor was controlled primarily by the peak pressure and the initial decay slope, an attenuation factor for roof-depth level was estimated, on the basis of the aforementioned 5000-psi, 1.0 KT pulse, to be about 0.8. Proceeding then, in the usual manner, the roof loading pulse shown in Fig. 14(a) was developed.

Resistance Function: The resistance function for this case, determined as described for earlier analyses, was found to be the same as the resistance for Mighty Mach No. 1. It is reproduced here for convenience as Fig. 14(b).

The Natural Period remains 1.77 ms, as determined for the immediately preceding analysis.

Results: For the model just described, the maximum deflection was computed to be 7.0 inches, which should be compared with the complete collapse of the roof that was observed in the test. As to whether the computational procedure is confirmed by the test results is not entirely clear, but a deflection of 7.0 inches in a span of only 16 inches would certainly appear to be approaching a collapse condition.

As was done for the first Mighty Mach case, the effects of the pressure attenuation uncertainty were studied also for this second Mighty Mach case, and it was studied in precisely the same way in which it was studied in the first case.

Assuming that the ground surface pressure function was the overpressure produced at a range of 3.79 ft by a 0.0009 KT weapon at an HOB of 10 ft, the pressure attenuation factor is determined to be about 0.25, and the roof loading function developed therefrom is as shown in Fig. 15(a). For the same reasons that were discussed in the first Mighty Mach case, this probably underestimates somewhat the magnitude of the attenuation factor, since the surface pulse assumed here has an initial decay slope that is less steep than is the zero-HOB pulse that is assumed in the attenuation-factor plot that was used in this determination.

Neither the resistance function, which is shown in Fig. 15(b), nor the period of vibration was changed as a consequence of this change in surface loading, and the maximum response of this revised loading case was found to be 6.1 inches. This suggests, as did the corresponding comparative analysis that was run for the first Mighty Mach test, that the response of this model is sensitive not so much to the shape of the loading function but primarily to the total impulse that is contained in it.

1.5.7 Summary of Results.

To facilitate comparison and interpretation, the results that were obtained in this study are summarized below.

For Foam HEST 4 - A Quarter-Scale, Single-Bay Model:

The surface loading is reasonably approximated by the overpressure pulse whose peak value is 1900 psi from a 0.85 KT weapon detonated on the ground surface.

The observed maximum deflection was 12.5".
The computed maximum deflection was 15.2".

Parametric variation studies showed that:

If C_a = 0.80 instead of 0.85, x_m = 14.2"
If α_z = 0.80 instead of 0.70, x_m = 13.9"
If T = 5.3 ms instead of 5.8 ms, x_m = 14.1"

For Foam HEST 7 - A Quarter-Scale, Three-Bay Model:

The surface loading is reasonably approximated by the overpressure pulse whose peak value is 2360 psi from a 1.2 KT weapon detonated on the ground surface.

The observed maximum deflection was complete collapse. The computed maximum deflection was 18.5". (The computer program used in the analysis has no criterion for collapse, but a deflection of 18.5" in a clear span of only 48" is certainly large enough to constitute complete failure, and if realized physically, might well have entailed complete collapse.)

No parametric variations were considered for this case.

For Dynamic Shear Test No. 3 - A Quarter-Scale, Single-Bay Model:

The surface loading is reasonably approximated by the overpressure pulse whose peak value is 3330 psi from a 0.23 KT weapon detonated on the ground surface.

The observed maximum deflection was 9.5" to 11.5".
The computed maximum deflection was 15.2".

Parametric variation studies showed that:

If C_a = 0.71 instead of 0.78, x_m = 14.0"
If T = 6.6 ms instead of 5.6 ms, x_m = 13.1"
If both C_a and T are changed as noted, x_m = 12.0"

For FY-85 Half-Scale Test - A Half-Scale, Single-Bay Model:

The surface loading is reasonably approximated by the overpressure pulse whose peak value is 1284 psi from an 89.8 KT weapon detonated on the ground surface.

The observed maximum deflection was about 50", of which only about 44" were attributed to roof slab deformation. The computed maximum deflection was 36.4"

Parametric variation studies showed that:

If α_z = 0.90 instead of 0.85, x_m = 37.8"
If C_a = 0.90 instead of 0.85, x_m = 38.9"
If T = 11.8 ms instead of 10.8 ms, x_m = 34.6"
If T = 9.8 ms instead of 10.8 ms, x_m = 38.4"

If the initial spike of increased resistance that results from in-plane force amplification is neglected, x_m = 39.6"

For Mighty Mach Test No. 1 - A Twelfth-Scale, Single-Bay Model:

The surface loading was taken as the average of two over-pressure records whose peak values differed by about 25 percent and whose total impulses differed by about 40 percent. The resulting function had a peak value of 2700

psi, a duration of 2.0 ms, and a total impulse of 1053 psi-ms. This pulse could not be reasonably represented by an equivalent nuclear blast, but its pressure attenuation factor was estimated on the basis of its peak pressure and a weapon yield that reasonably approximated its initial decay rate.

The observed maximum deflection was 1.75".
The computed maximum deflection was 4.6".

While the average surface pressure function described above cannot be represented by an equivalent nuclear blast, its total impulse is reasonably reproduced by an overpressure pulse whose peak value is 5405 psi, produced at a range of 3.79' by a 0.0013 KT weapon detonated at an HOB of 15.0', which are the same range and HOB of the actual test. Using this surface load function and the associated pressure attenuation factor, the maximum deflection is computed to be 4.2".

For Mighty Mach Test No. 4 - A Twelfth-Scale, Single-Bay Model:

The situation for this test was very much like that of Mighty Mach No. 1 as described immediately above. Its surface loading was taken as the average of two overpressure records whose peak values differed by a factor of 2.3 and whose total impulses differed by a factor of 2.6. The resulting average function had a peak value of 5000 psi, a duration of 1.4 ms, and a total impulse of 1292 psi-ms. As in the previous case, this pulse could not be reasonably approximated by an equivalent nuclear blast, but its pressure attenuation factor could be estimated on the basis of its peak pressure and a weapon yield that was compatible with its initial rate of decay.

The observed maximum deflection was total collapse.
The computed maximum deflection was 7.0".

If the surface loading is taken as the impulse-equivalent overpressure pulse produced at a range of 3.79' from an HOB of 10' (the range and HOB of the actual test), the peak pressure will be 12,136 psi and the "equivalent" weapon yield will be 0.0009KT. Using this pulse as the surface load and its associated attenuation factor, the maximum deflection is computed to be 6.1".

1.5.8 Discussion of Results.

Since the computational procedures employed in these analyses were developed on the basis of the quarter-scale SBS test series, it was to be expected that the computed results for the Foam HEST 4, Foam HEST 7,

and Dynamic Shear Test No. 3 would agree quite well with the maximum deflections that were observed in those tests. And such was the case. Although the computed maximum deflections of those structures differed somewhat from the observed test values, these differences were quite small in comparison with the observed maxima, especially when the potential effects of relatively small variations in some of the more uncertain but significant parameters are taken into account. Indeed, it would appear that these results served to confirm the applicability of this analytical model to structures of this type and of this relative size.

And much the same thing can be said in regard to the half-scale test of FY-85. Computed maxima of from 35 to 40 inches, depending upon the assumptions that are made in regard to some of the more uncertain parameters, would appear to agree quite well with a measured deflection of about 44 inches. Hence, there is no evidence in these results to suggest that significant scale effects exist between the quarter-scale and half-scale models.

But the situation in regard to the twelfth-scale models of the Mighty Mach test series is not so clear. For Test No. 1 of that series, the computed deflection is sufficiently large in comparison with the observed value (4.6" vs 1.75") to suggest that scale effects may be important at scales as small as this. But the results of the analyses of Test No. 4 of that series would suggest that if such scale effects did occur in this test, they acted in a fashion contrary to the way in which they acted in the first test of the series, since, for Test No. 4, the structure suffered complete collapse, while the computed maximum deflection was found to be about 7.0 inches.

Actually, a deflection of 7.0 inches in a span of only 16.0 inches is tantamount to collapse, and if only Test. No. 4 had been run, it could be argued that scale effects, even at this very small scale, are negligible, if they exist at all. But Test No. 1 was run and, in that test, the computed maximum deflection of 4.6" was relatively much larger that was the observed maximum deflection of only 1.75".

As to why the computed deflection is substantially larger than the observed deflection in Test No. 1, while it is less than or equal to

the observed deflection in Test No. 4, is not clear. But it is entirely possible that these differences may result from surface load definition uncertainties. The surface pressure functions for these two tests were taken as averages of quite widely varying measured overpressure pulses, which suggests the possibility of substantial inaccuracies in their determinations.

Even the second analysis that was made in each case, using a significantly different, but impulse-equivalent, surface pressure pulse, shed little additional light on this problem. They served only to show that the responses in this case are largely impulse-sensitive and, therefore, that the shapes of those impulses within their very short total durations are of little importance insofar as their influence of the maximum deflection is concerned.

Consequently, it must be concluded that the twelfth-scale model tests were inconclusive as far as scale effects were concerned. While they certainly did not establish the existence of significant scale effects at this small scale, neither did they confirm convincingly the insignificance of such effects. It is, however, clear that scale effects at the quarter- and half-scale levels are small, if they exist at all.

Table 1. Pressure-time data as read from the record of gage OP 0.0 from Mighty Mach Test No. 1.

TIME (ms)	[1]PRESSURE (psi)	ACCUMULATED IMPULSE (psi-ms) DATA[2]	CALCULATED[3]
0.0	3000	0	0
.1	2000	250	250
.2	1500	410	425
.3	1200	560	560
.4	1100	665	675
.5	900	740	775
.6	800	825	860
.7	700	905	935
.8	600	985	1000
.9	500	1060	1055
1.0	400	1115	1100
.1	300	1145	1135
.2	250	1170	1163
.3	200	1185	1185
.4	150 (?)		1202
.5	100 (?)		1215
.6	60 (?)		1223
.7	30 (?)		1227
.8	20 (?)		1230
.9	10 (?)		1231
2.0	0 (?)		1232

[1]Data beyond t=1.4ms are estimates necessitated by the fact that these data were to be averaged with similar data from Gage OP 7.W; Data as read from Fig. 9(a).

[2]Impulses as read from Fig. 9(a); No data beyond t = 1.4 ms.

[3]Impulses as computed from pressure data shown herein.

Table 2. Pressure-time data as read from the record of gage OP 7.W from Mighty Mach Test No. 1.

TIME (ms)	[1]PRESSURE(psi)	ACCUMULATED IMPULSE (psi-ms) [1]DATA	[2]CALCULATED
0.0	2400	0	0
.1	1600	175	200
.2	1200	305	340
.3	800	435	440
.4	700	500	515
.5	600	560	580
.6	500	625	635
.7	450	695	683
.8	400	740	725
.9	350	775	763
1.0	250	815	793
.1	200	835	815
.2	150	845	833
.3	120	855	846
.4	80	860	856
.5	60	862	863
.6	40	865	868
.7	20	868	871
.8	10	870	873
.9	5	875	873
2.0	0	875	873

[1]Data as read from Fig. 9(b).
[2]Data as computed from the pressure data tabulated herein.

Table 3. Estimated surface pressure function for Mighty Mach Test No. 1.

TIME (ms)	[1]EXPERIMENTAL PRESSURE (psi)	[1]EXPERIMENTAL IMPULSE (psi-ms)	[2]BRODE PULSE PRESSURE (psi)	[2]BRODE PULSE IMPULSE (psi-ms)
0.0	2700	0	5405	0
.1	1800	225	2537	397
.2	1350	383	1402	594
.3	1000	500	897	708
.4	900	595	601	782
.5	750	678	437	834
.6	650	748	331	872
.7	575	809	257	902
.8	500	863	205	925
.9	425	909	166	943
1.0	325	946	136	958
.1	250	975	112	971
.2	200	998	94	981
.3	160	1015	79	990
.4	115	1029	67	997
.5	80	1039	57	1003
.6	50	1045	49	1008
.7	25	1049	42	1013
.8	15	1051	36	1017
.9	7	1052	31	1020
2.0	0	1053	27	1023
3.0	0	1053	8	1038
4.0	0	1053	2	1043
5.6	0	1053	0	1044

[1]Averages of the data given in Tables 1 and 2.

[2]Computed as the overpressure pulse at R = 3.79 ft. from W = 0.0013KT at HOB = 15.0 ft.

Table 4. Pressure-time data as read from the record of gage OP 0.0 from Mighty Mach Test No. 4.

TIME (ms)	[1]PRESSURE (psi)	ACCUMULATED IMPULSE (psi-ms) DATA[1]	CALCULATED[2]
0.0	7000	0	0
.1	4500	435	575
.2	3000	900	950
.3	2000	1200	1200
.4	1500	1380	1375
.5	1100	1510	1505
.6	850	1620	1602
.7	700	1690	1680
.8	550	1740	1742
.9	400	1780	1790
1.0	300	1810	1825
.1	200	1835	1850
.2	100	1860	1865
.3	50	1870	1872
.4	0	1875	1875

[1]Data as read from the record of Fig. 10(a).

[2]Computed from the pressure data tabulated herein.

Table 5. Pressure-time record as read from the record of gage OP 8.0 from Mighty Mach Test No. 4.

TIME (ms)	[1]PRESSURE (psi)	ACCUMULATED IMPULSE (psi-ms) DATA[1]	CALCULATED[2]
0.0	3000	0	0
.1	1500	200	225
.2	1100	330	355
.3	800	440	450
.4	600	520	520
.5	450	580	573
.6	350	615	613
.7	250	650	643
.8	200	670	666
.9	150	685	683
1.0	100	700	696
.1	60	705	704
.2	30	710	708
.3	0	715	710

[1]Data as read from Fig. 10(b).

[2]Computed from the pressure data tabulated herein.

Table 6. Estimated surface pressure function for Mighty Mach Test No. 4.

TIME (ms)	[1]EXPERIMENTAL PRESSURE (psi)	[1]EXPERIMENTAL IMPULSE (psi-ms)	[2]BRODE PULSE PRESSURE (psi)	[2]BRODE PULSE IMPULSE (psi-ms)
0.0	5000	0	12136	0
.1	3000	400	3067	760
.2	2050	652	1351	981
.3	1400	825	774	1087
.4	1050	948	499	1151
.5	775	1039	344	1193
.6	600	1108	247	1223
.7	475	1162	183	1244
.8	375	1204	139	1260
.9	275	1237	108	1273
1.0	200	1261	85	1282
.1	130	1277	68	1290
.2	65	1287	55	1296
.3	25	1291	45	1301
.4	0	1292	37	1305
.5	0	1292	31	1308
2.0	0	1292	13	1319
3.0	0	1292	3	1326
4.0	0	1292	1	1328
5.6	0	1292	0	1329

[1]Averages of the data given in Tables 4 and 5.

[2]Computed as the overpressure pulse at R=3.79 ft. from W = 0.009 KT at HOB = 10.0 ft.

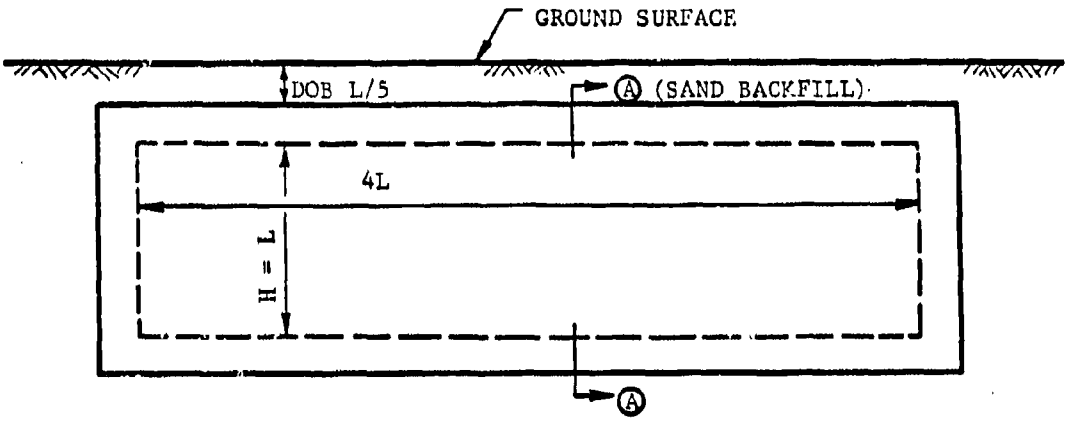

(a) Side Elevation View

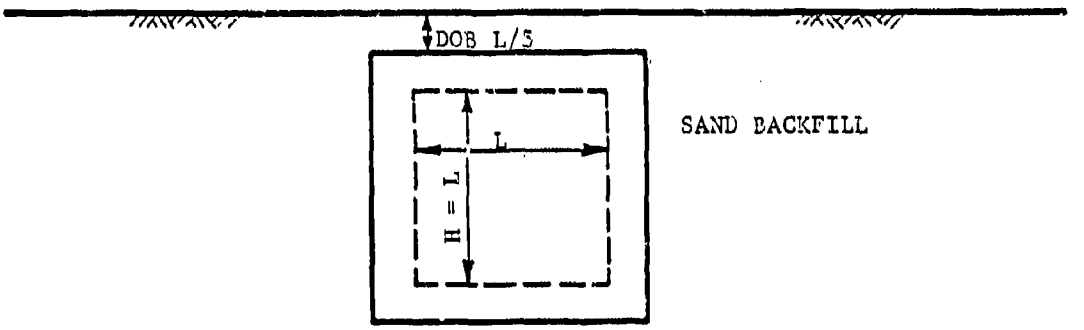

(b) Section A-A for Single Bay Model

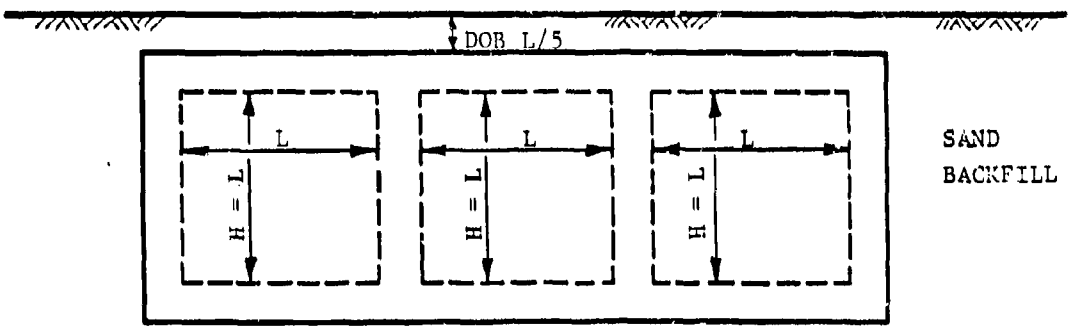

(c) Section A-A for Three-Bay Model

Figure 1. Typical model test structures.

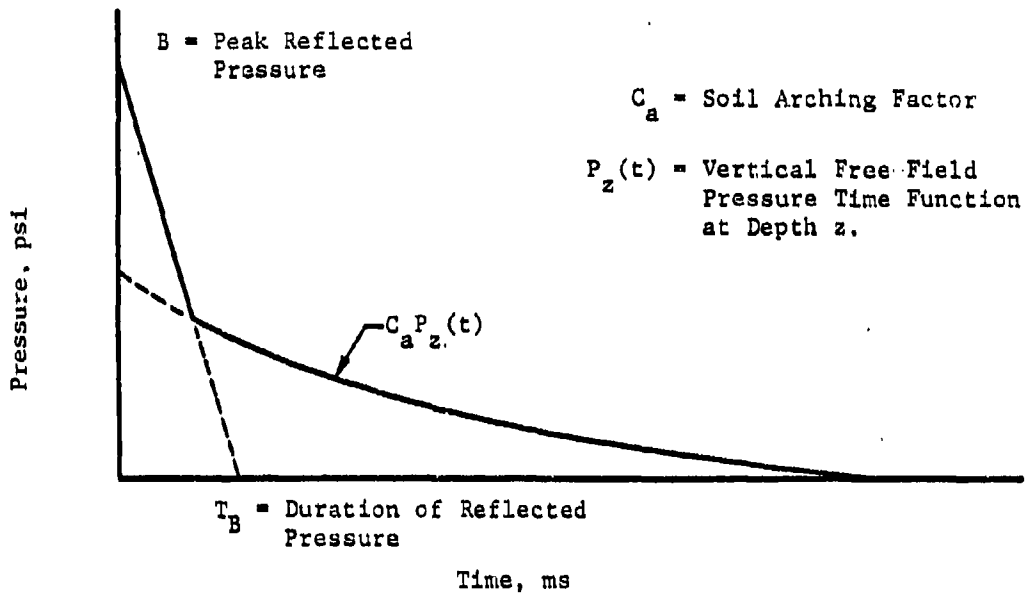

Figure 2. Typical roof loading function.

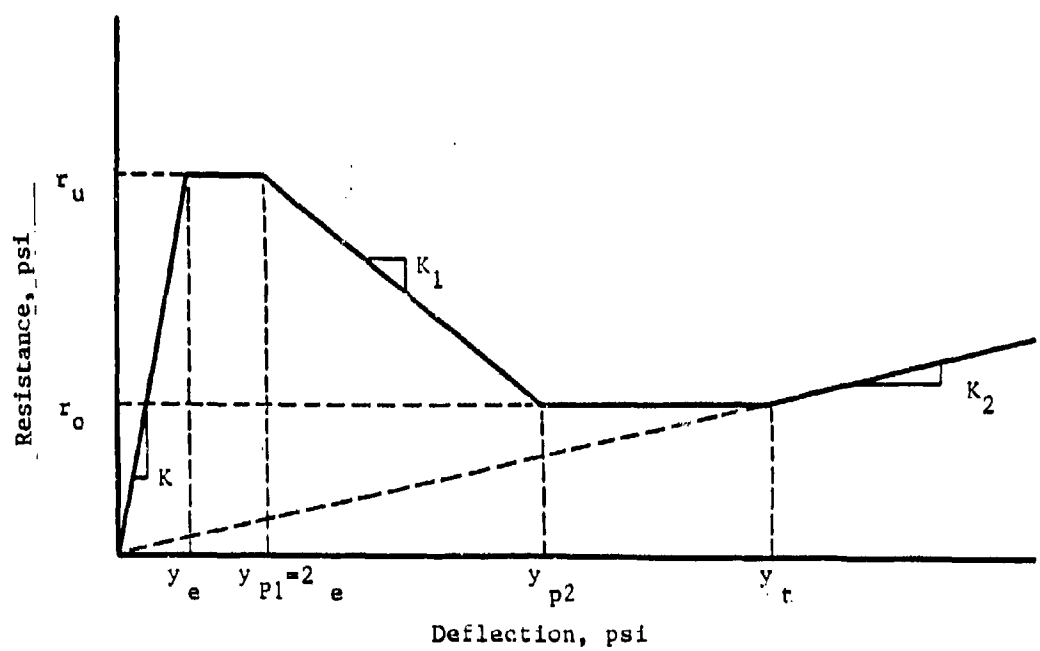

Figure 3. Typical resistance function.

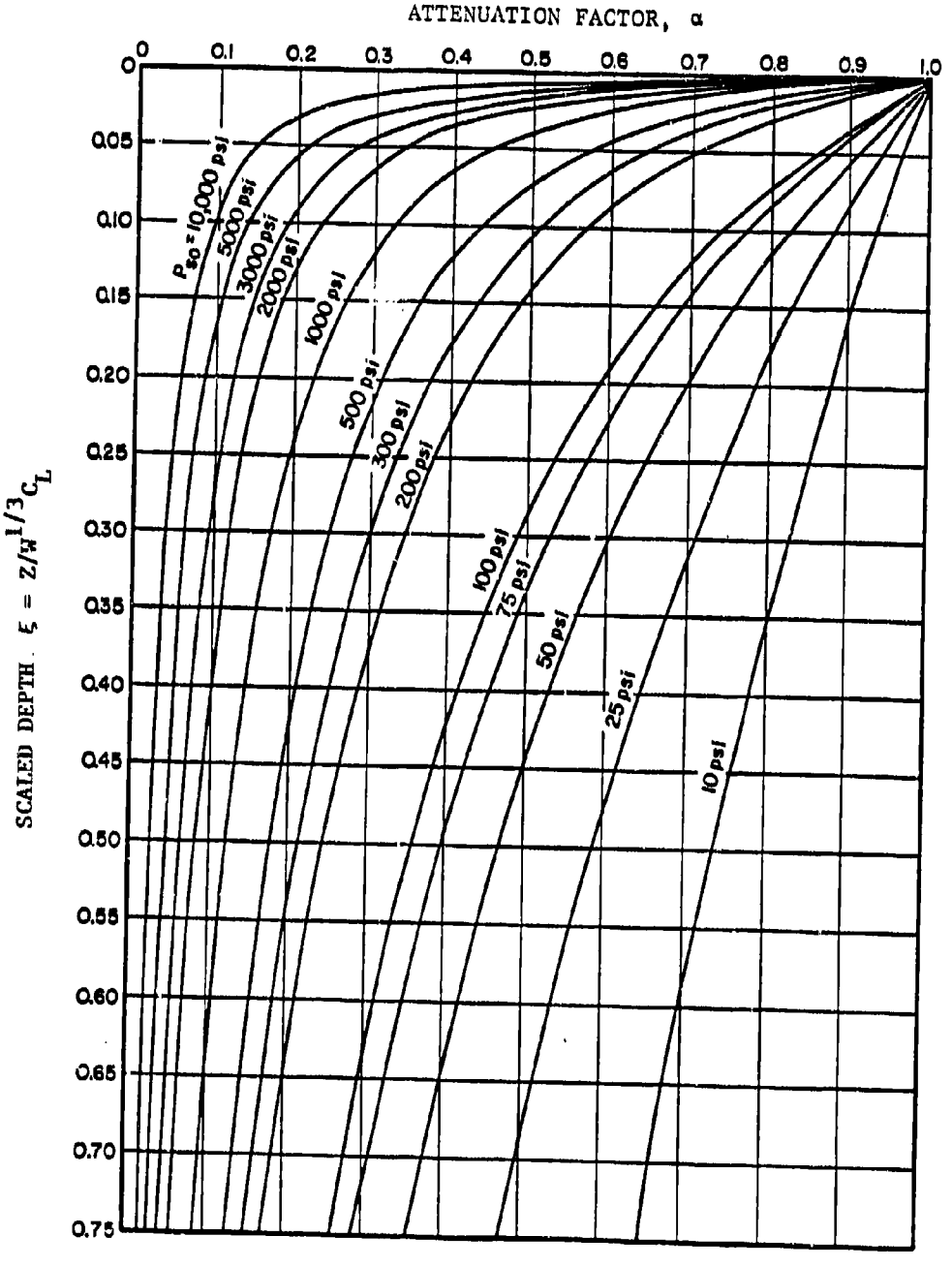

Figure 4. Attenuation factor versus scaled depth for bilinear model, r = 1/10 (from Ref. 7).

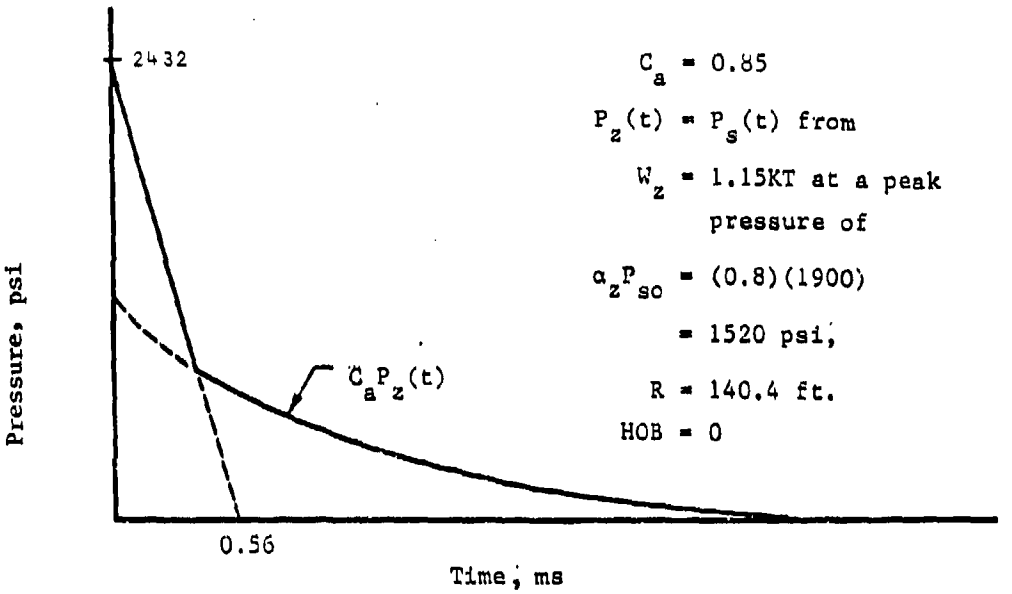

(a) Roof Loading Function

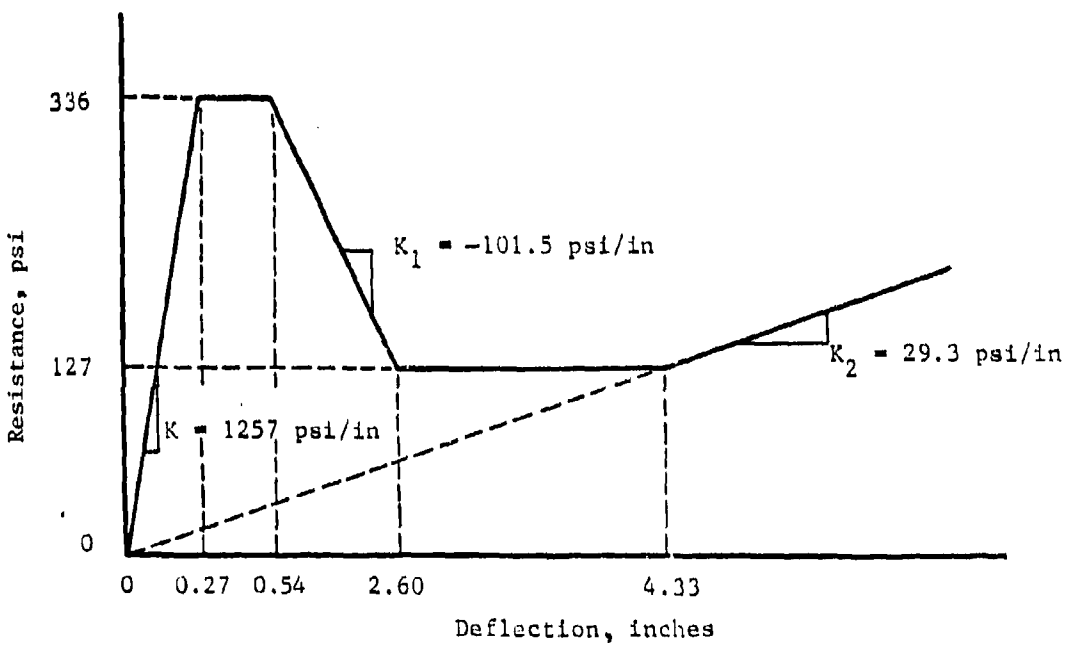

(b) Resistance Function

Figure 5. Roof loading and resistance functions for Foam Hest 4.

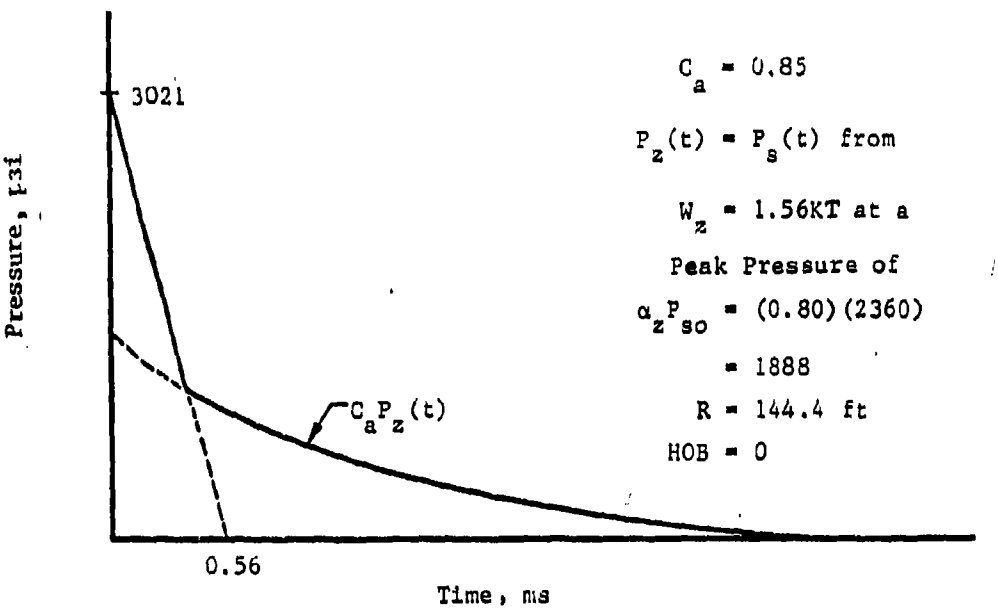

(a) Roof Loading Function

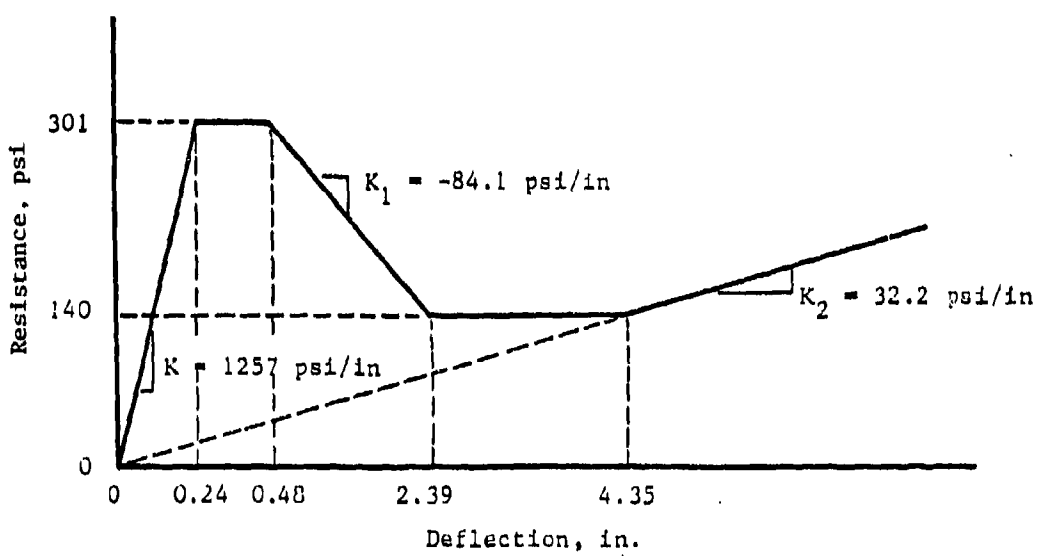

(b) Resistance Function

Figure 6. Roof loading and resistance functions for Foam Hest 7.

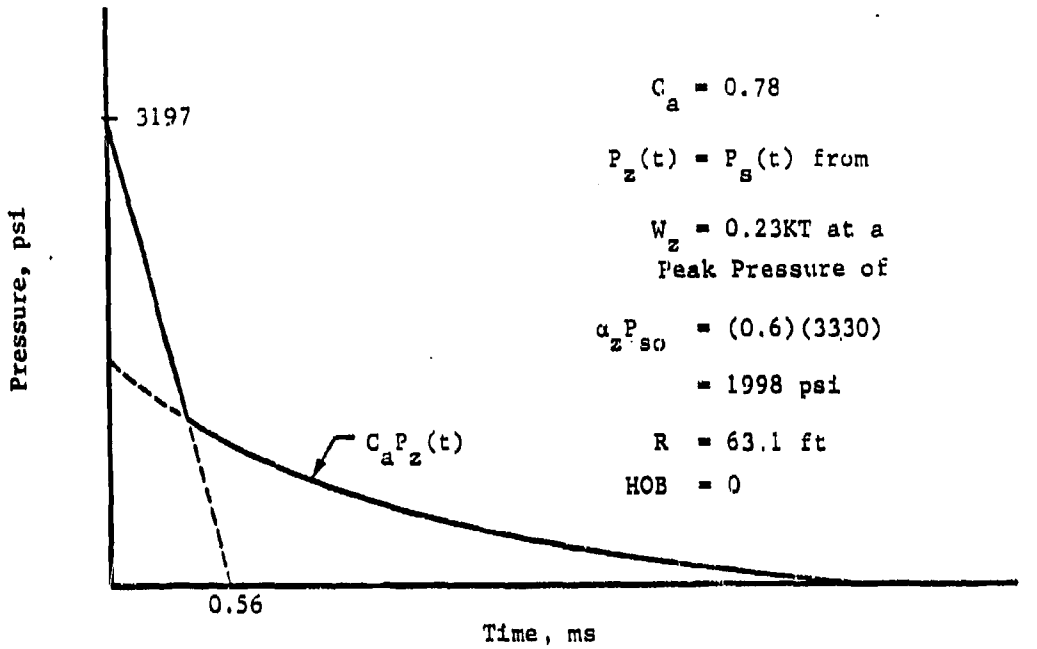

(a) Roof Loading Function

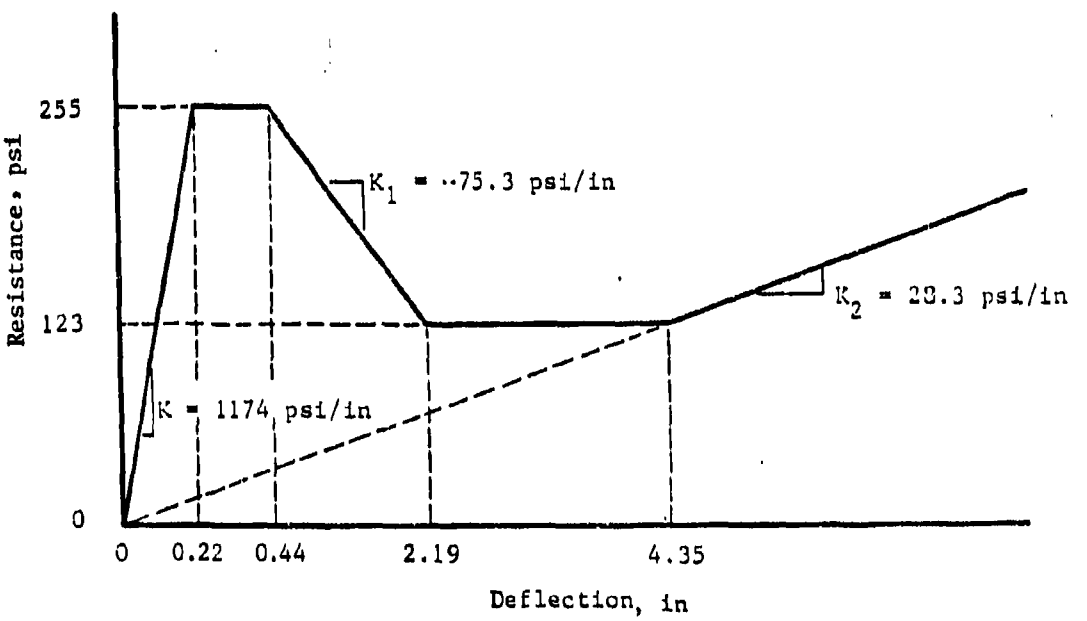

(b) Resistance Function

Figure 7. Roof loading and resistance functions for Dynamic Shear Test No. 3.

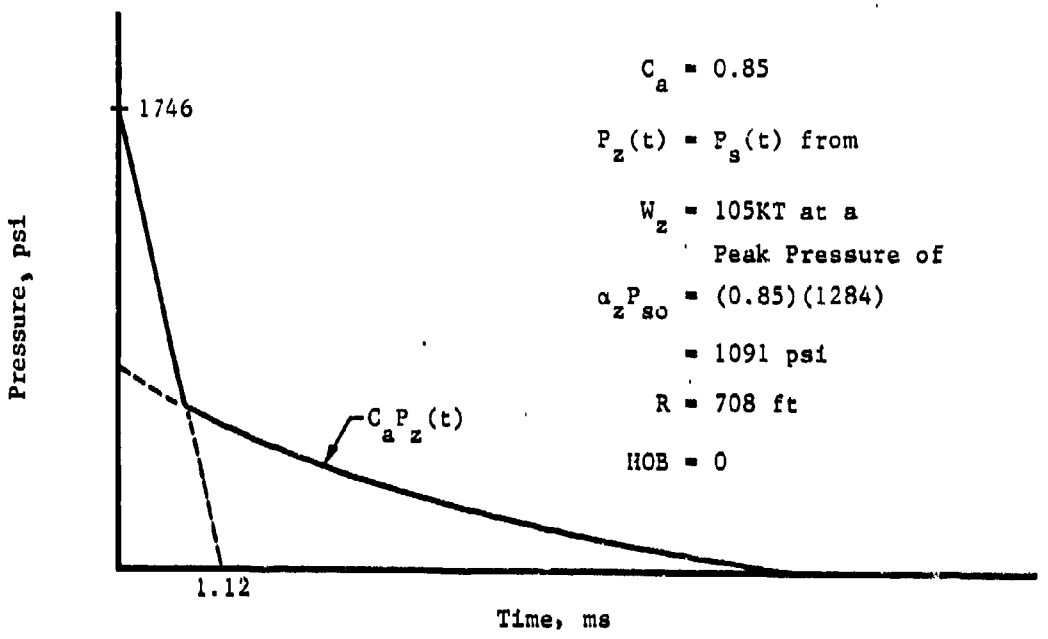

(a) Roof Loading Function

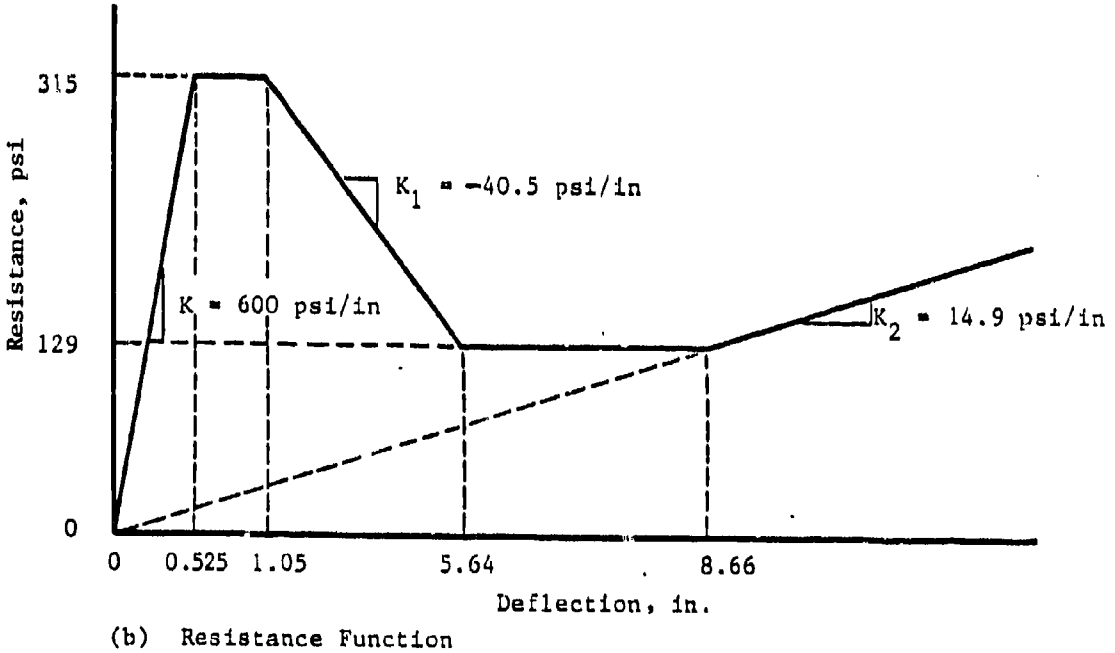

(b) Resistance Function

Figure 8. Roof loading and resistance functions for FY-85 Half-Scale Test.

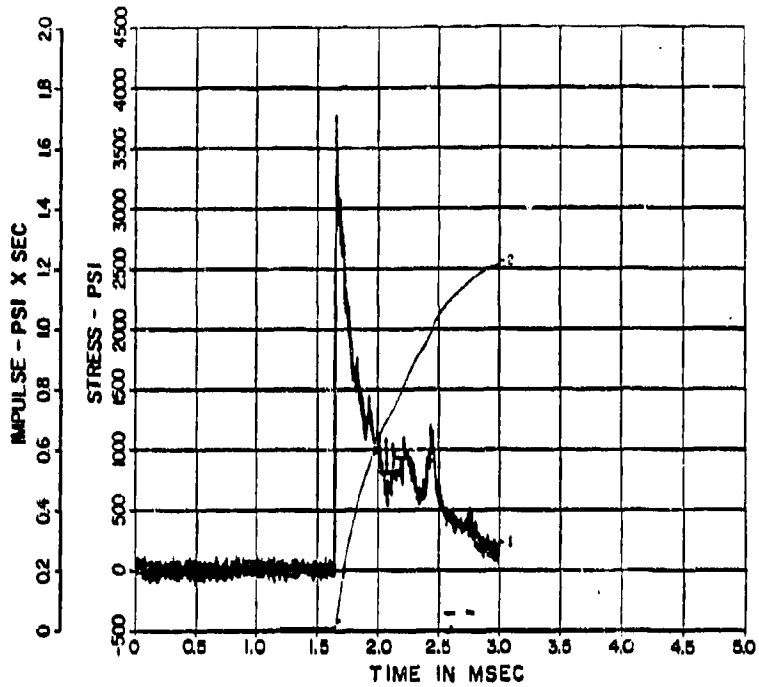

(a) Pressure Record OP 0.0

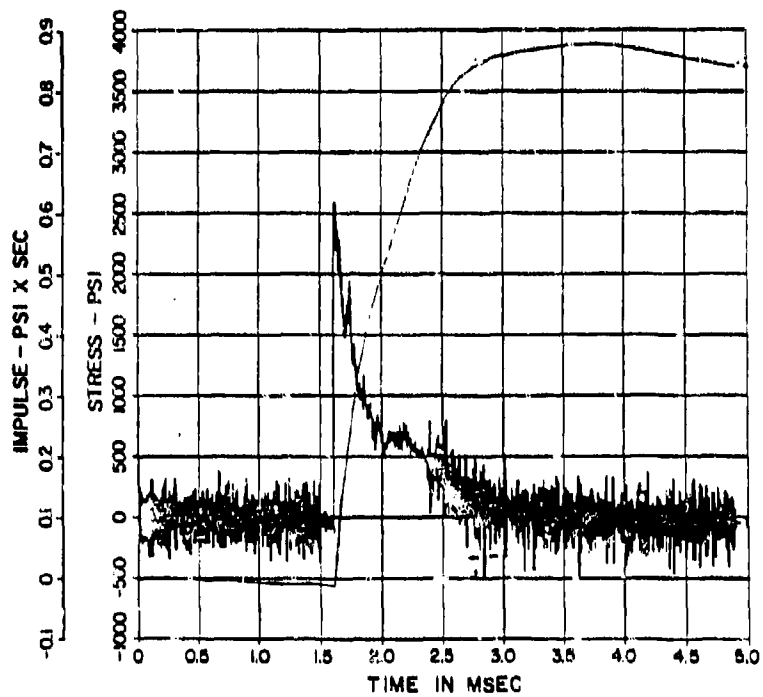

(b) Pressure Record OP 7.W

Figure 9. Surface overpressure records for Mighty Mach Test No. 1 (from Ref. 9).

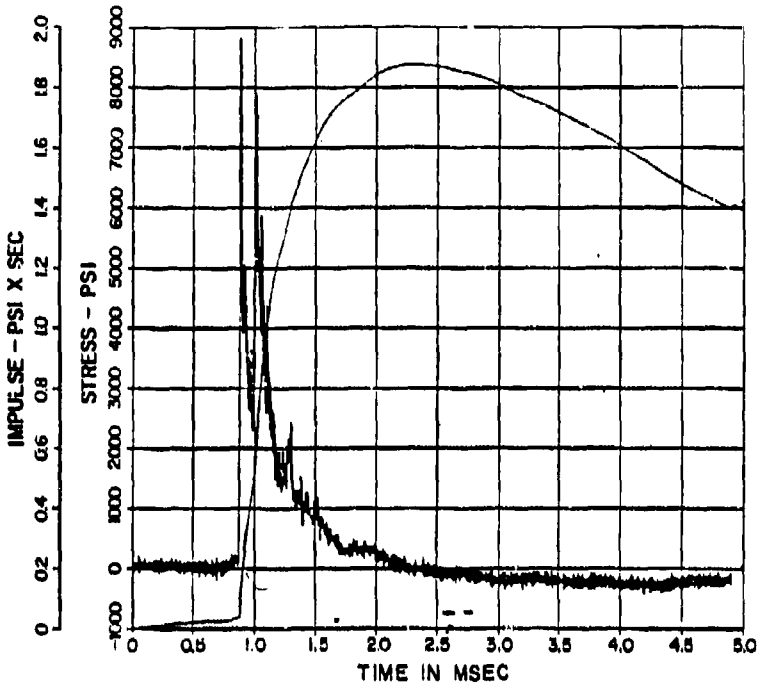

(a) Pressure Record OP 0.0

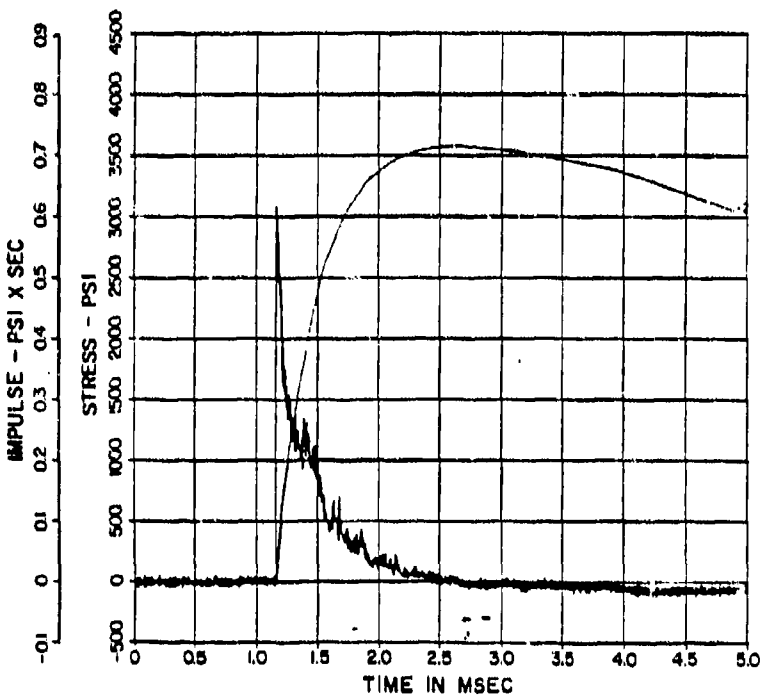

(b) Pressure Record OP 8.0

Figure 10. Surface overpressure records for Mighty Mach Test No. 4 (from Ref. 9).

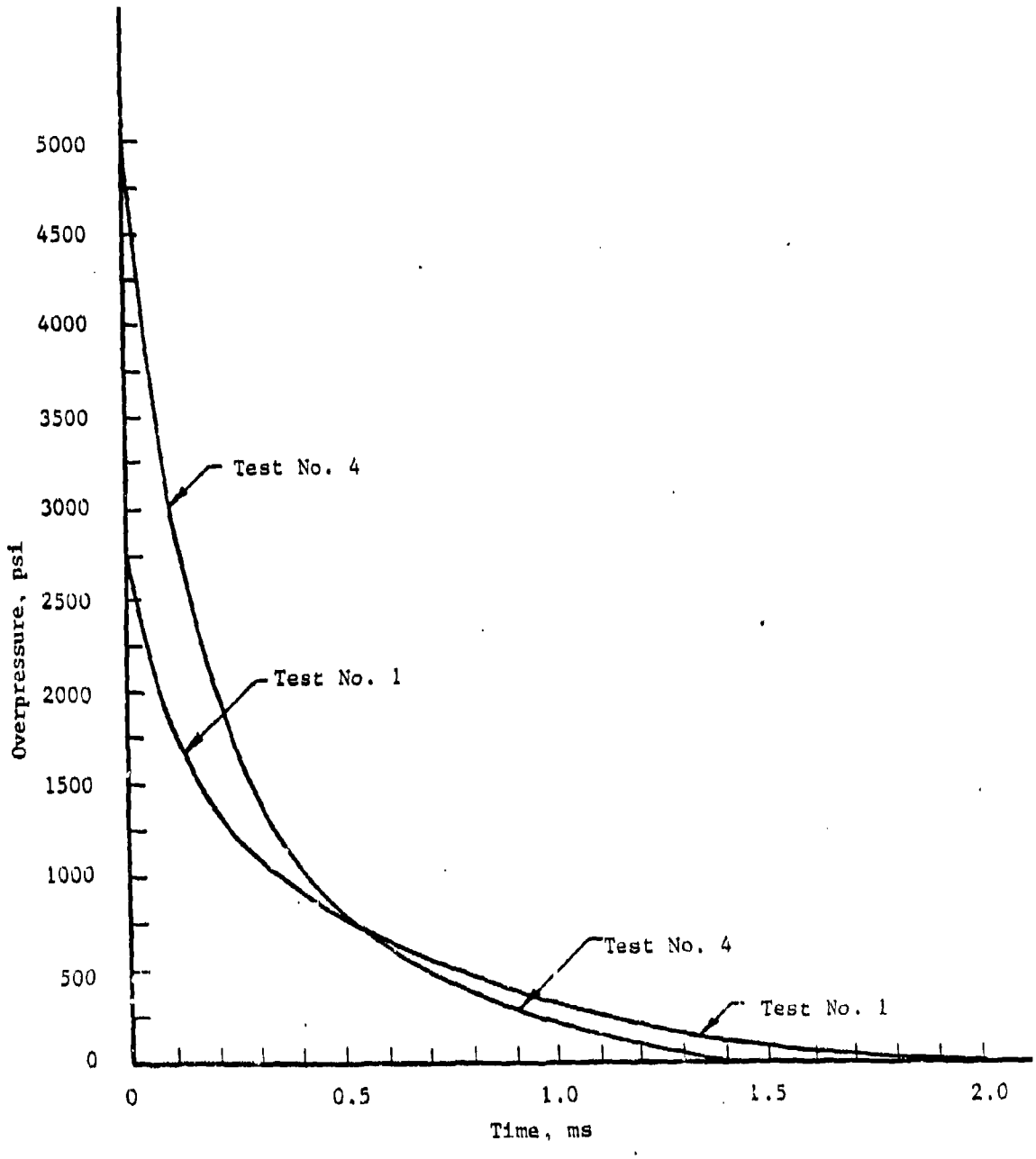

Figure 11. Estimated surface pressure functions for Mighty Mach Tests 1 and 4.

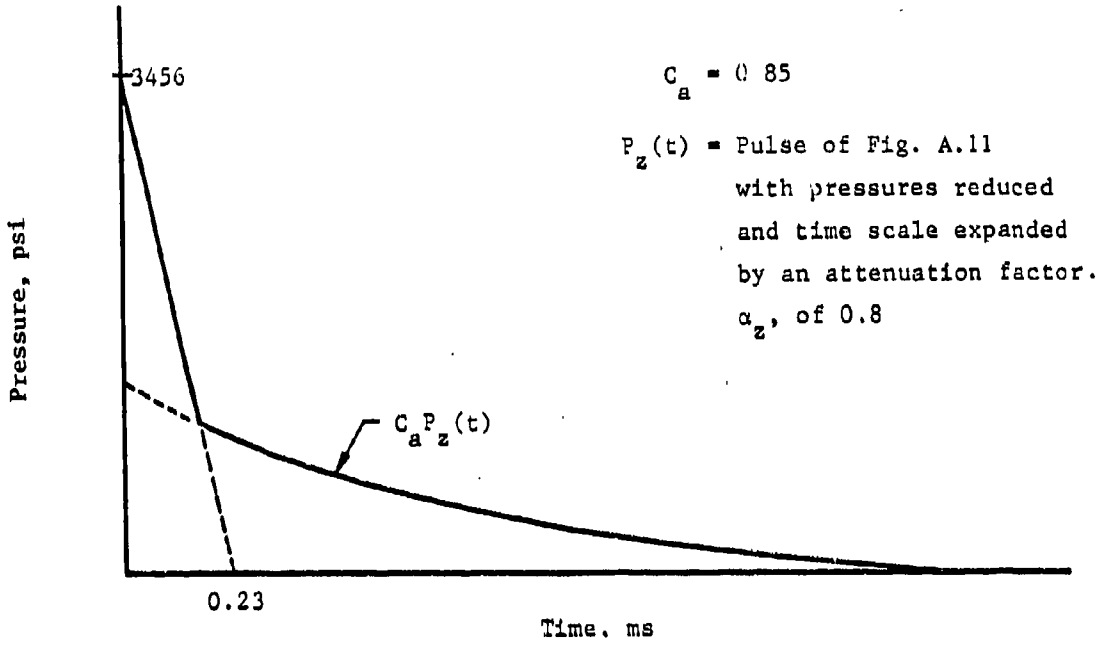

(a) Roof Loading Function

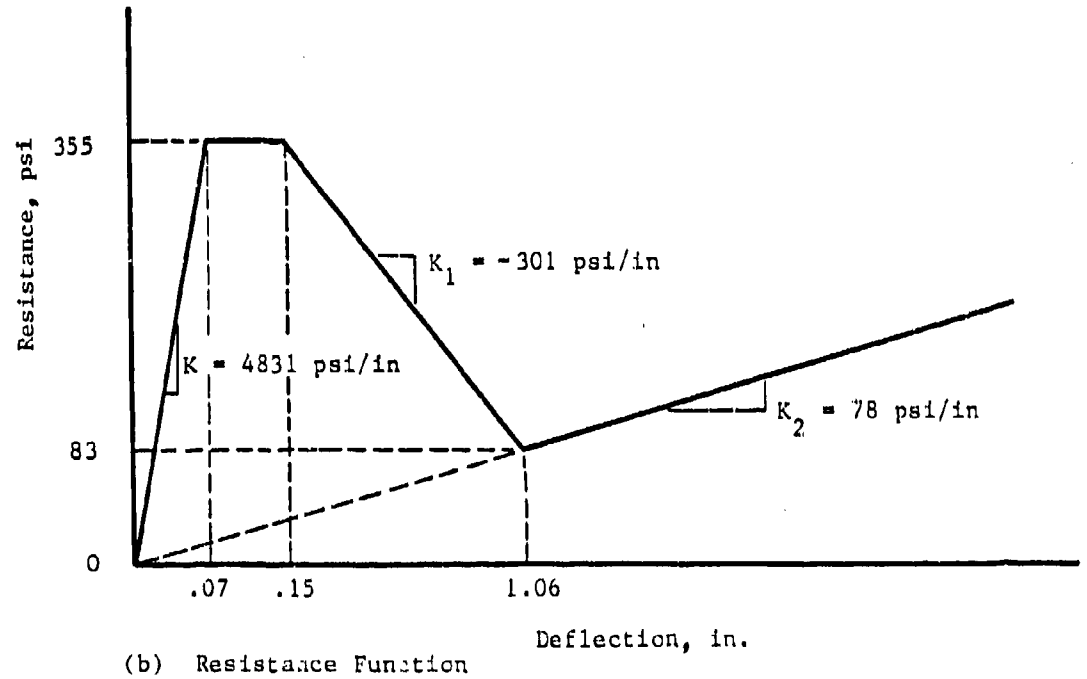

(b) Resistance Function

Figure 12. Roof loading and resistance functions for Mighty Mach Test No. 1.

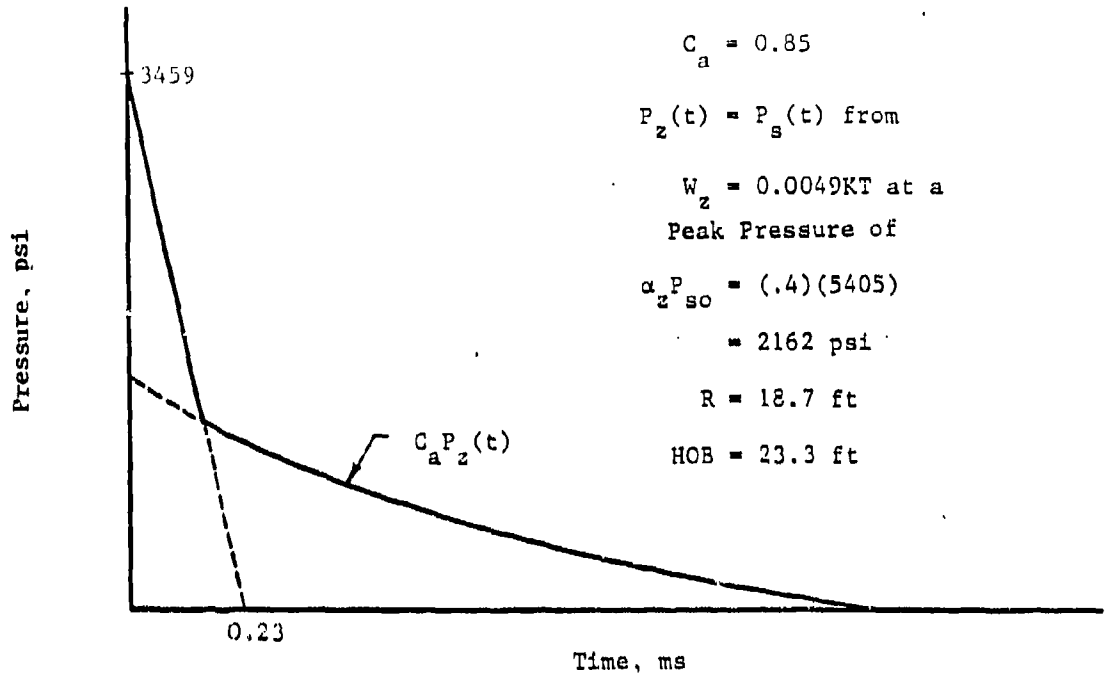

(a) Roof Loading Function

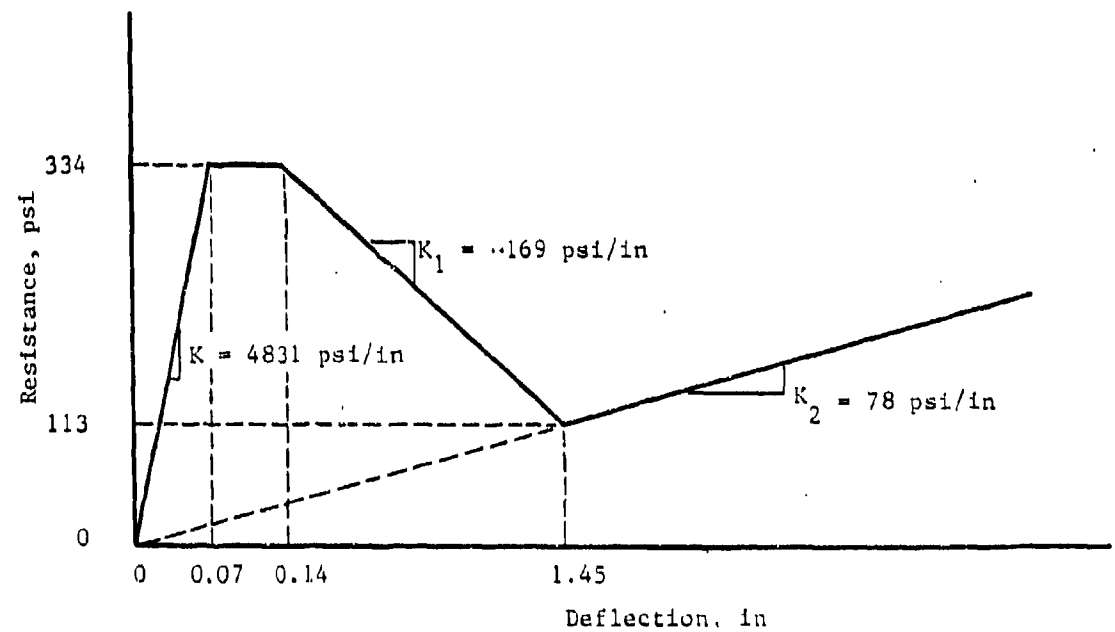

Figure 13. Modified roof loading and resistance functions for Mighty Mach Test No. 1.

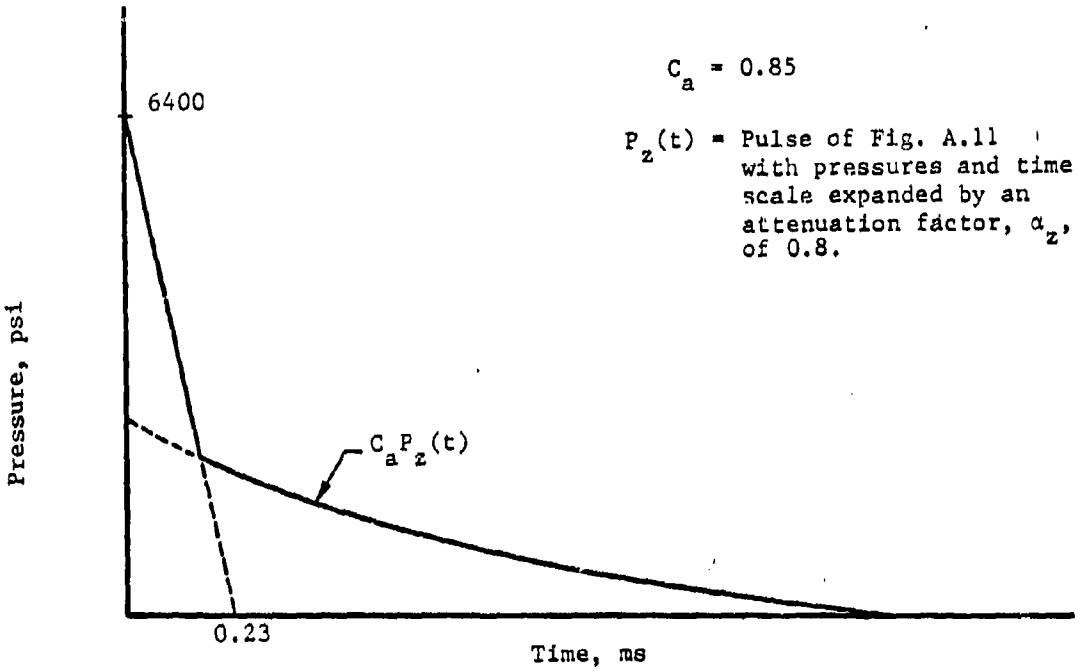

(a) Roof Loading Function

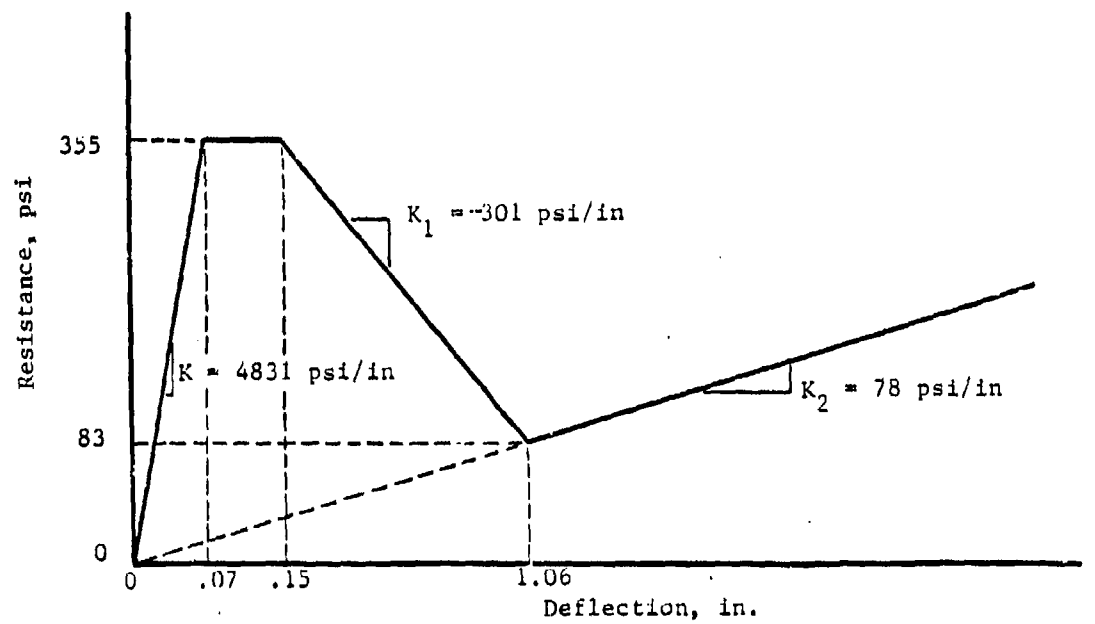

(b) Resistance Function

Figure 14. Roof loading and resistance functions for Mighty Mach Test No. 4.

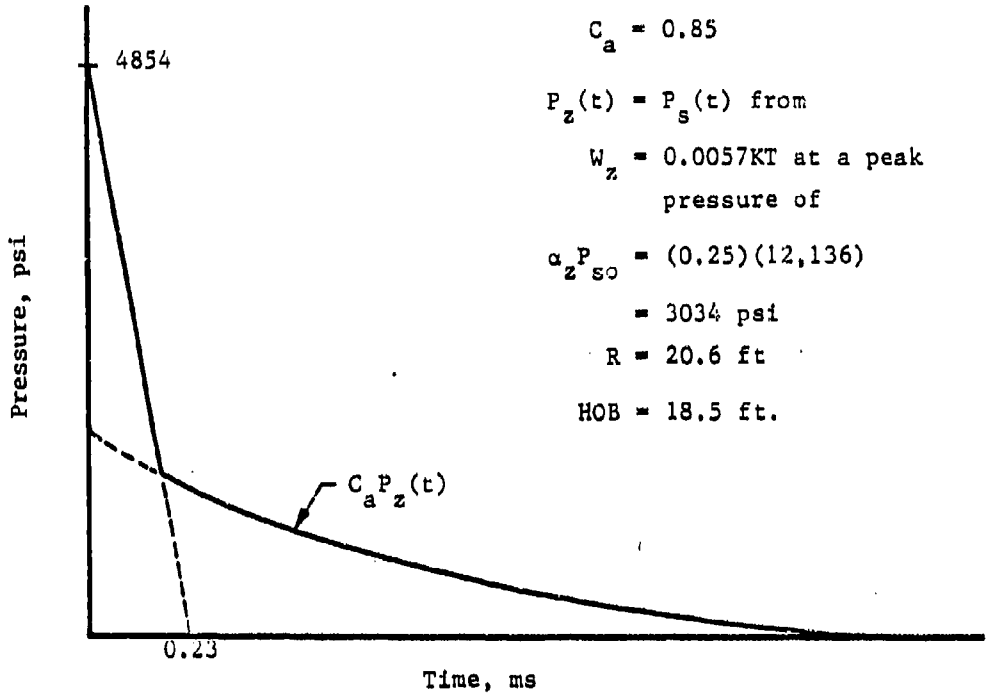

(a) Roof Loading Function

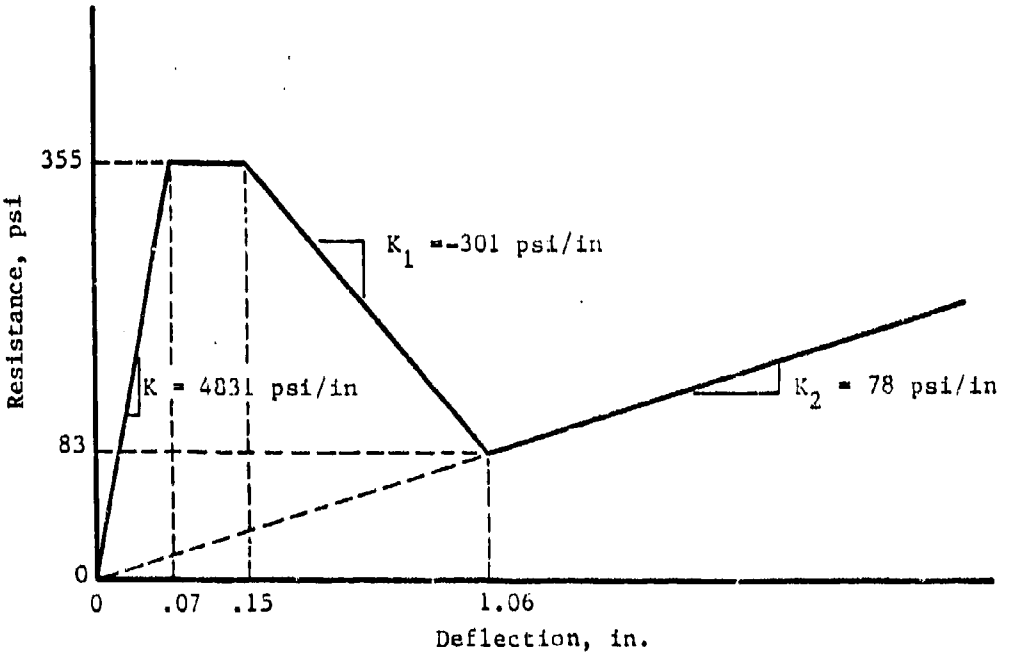

(b) Resistance Function

Figure 15. Modified roof loading and resistance functions for Mighty Mach Test No. 4.

SECTION 2
CRITERIA CONSIDERATIONS FOR SHOCK EFFECTS ON GROUND SUPPORTED EQUIPMENT

2.1 FOREWORD.

This section of the report centers on the topic of the effect of base excitation on the response of ground supported equipment, and, more specifically on design/analysis criteria for such effects. Although much has been written on the topic in recent years, there is a perceived need to attempt to consolidate in one document the principles, conditions and criteria that are applicable in the context of current military design and analysis environments, environments that, in many cases, are much different than those of a decade ago.

Over the years, in designing protective facilities with their included mechanical and electrical equipment, or alternatively carrying out physical vulnerability analyses of such targets, the topic has received considerable, yet not a great deal of attention. In many cases, major attention has been centered on design techniques surrounding "shock isolation", defined in its most generic sense, and alternatively from the physical vulnerability point of view, on techniques for overcoming the shock isolation and for effecting damage to the equipment.

Some of the most sophisticated work in shock isolation has centered around ICBM missile systems, and ships and submarines. This document does not attempt to summarize such work in detail, in part since much of it is sensitive and thereby classified; however, it is appropriate to note that in those cases where major shock excitation of large weapons has been a design criterion, as for example large ICBM systems, complex large-scale shock isolation systems have been employed. The design details and design criteria for such systems are not the subject of this document, except for some brief comments when discussing ground shock input; this document centers attention on input and design/analysis criteria applicable to closely-supported (not shock isolated) ground-mounted equipment.

Also in the last two decades, with the advent of major critical facilities such as nuclear power plants and offshore oil platforms that must be designed for earthquake resistance, there has been increased attention given to earthquake excitation effects on equipment fragility. It was this type of work that led to development of the basic theory on energy dissipation in simple nonlinear systems, as developed in additional detail for military systems in Refs. 11 and 12.

In spite of all of the foregoing, at present there is no definitive document specifically devoted to protective systems (structures and equipment) that outlines the principles and criteria applicable to evaluation of shock effects on ground supported equipment, especially as it pertains to situations characterized by the intense dynamics associated with current nuclear weapons effects. Thus, Section 2.2 of the report addresses criteria related considerations in the generic sense, outlines overall principles and considerations that would enter into basic equipment design, or alternatively as the first step in vulnerability analysis assessment.

Thereafter follows, in Section 2.3, a brief description of the types of ground supported equipment that might be envisioned as requiring this type of design attention. A listing of the environments (factors that are the sources of "loadings" and that also can affect the "resistance characteristics" in many cases) that need to be considered, singly or in combination, with applicable observations as to importance, is presented in Section 2.4. Section 2.5 contains a brief discussion of equipment mounting and brief observations on resistance and damage mechanisms. A discussion on the characterization of shock motions is presented in Section 2.6, including observations of shock spectra, as well as their uses and limitations. Section 2.7 treats briefly the subject of analysis approaches, Section 2.8 provides an overview on shock testing, and Section 2.9 is a concluding section offering some observations pertaining to design.

This brief listing of the scope is indicative of the complex nature of the shock design/analysis situation. It is hoped that the detailed overview that follows will be of aid to designers and analysts on future activities in this area; also, it is envisioned that it may

be desirable to update the document from time to time in order to maintain a current guideline on the subject that will be of use generally to others.

2.2 DESIGN CRITERIA -- GENERAL OVERVIEW.

In establishing design criteria it is important that first there be a clear description of the object under consideration and its role in the system being designed. This description normally includes a definition of the physical characteristics of the equipment, i.e., makeup of the unit, dimensions, expected mounting and anticipated physical location of the system. But of equal importance is the matter of defining the function of the equipment item. What does it do? Does it operate for long periods of time, or for intermittent periods? Must it run during and after an attack? What happens if it is put out of service? And, an important point is to describe the various modes of damage that would cause it to be unusable or to malfunction.

Related to these points is the matter of maintenance. Are there environments over the long term that will make the equipment items more susceptible to damage or failure? This point is usually overlooked in establishing design criteria and in following through in the design, procurement and construction. A case in point pertains to the Davis Besse Nuclear Power Plant malfunction on 9 June 1985 where a relief valve failed to function properly and stuck open for the second time at this plant. To succinctly make the point, the relief valve operation was required because the No. 1 main feedwater pump malfunctioned; thereafter, so did the No. 2 main feedwater pump; and, thereafter, so did the two auxiliary feedwater pumps (Ref. The Blade, Toledo, OH, June 16, 1985, pp. B-1 - B-2). A later USNRC report cited 14 mechanical failures that actually occurred, all of which were recognized and, fortunately, overcome by the plant operators, thereby avoiding a serious accident. Incidentally, had an earthquake occurred at that time, with its attendant shock effects, one can envision blame for the malfunctions being leveled, at least initially, on the shaking. But such was not the case and this incident dramatizes the problem of "aging", i.e., the degradation of functionability of equipment after

being in use for sometime, or on standby. Even routine periodic checking (maintenance routines) may not guarantee the "robustness" and "ready status" of a piece of equipment. This topic of equipment functionability, especially as an element in a system is not well understood and deserves detailed thought by system designers and operators.

In considering functionability, one needs to consider all of the possible environments or loading conditions, singly or in various combinations, that can reasonably be expected to occur. But also one must consider "overload conditions" corresponding to possible exceedance conditions. In other words, if the design environment is exceeded for some reason, will the equipment item cease to function? Or, under such conditions, is its need immaterial? Clearly all alternatives need to be considered early in the design process in a systematic and rational manner.

Thus, in summary, the design criteria for shock must include detailed consideration of the environments to which the item and its components, as well as the system of which it is a part, may be subjected from the standpoint of the "design" conditions, long term operation ("aging"), and possible overload. On the resistance side, the design criteria should include descriptive material that will aid the designers in establishing the mounting of the unit, as well as providing the basis for assessment of the strength of the item in a gross sense as well as internal components, and in assessing those "loading" effects (environmental conditions) and responses that will affect functionability or contribute to damage. In this latter case, it is quite important to clearly define potential identifiable types of damage, as for example, yielding of rotating shifts, broken connectors, internal unit malfunction (mechanical or electrical), relay or component chatter, sheared bolts or welds, relative distortion of components, susceptibility to fatigue, etc.

Finally, there may be the matter of economics, including consideration of the funds that can be allocated to design, procurement, validation, etc. This topic may influence some of the foregoing considerations, and may well impact the constructability or

system requirements from a gross point of view. In other words, if the cost of the component is too great, it may be necessary to reevaluate the overall system and its components in light of function, mode of response under attack, etc. and to consider alternative designs.

It should be clear that design criteria are not easily drafted, require great study and thought, normally require revision and rerevision, and, if properly drafted, often will function as perhaps the principal "design tool".

To a large degree, much of the material that follows hereafter should, in some form, be reflected in the design (or analysis assessment) criteria document.

2.3 TYPICAL TYPES OF GROUND SUPPORTED EQUIPMENT.

Ground support equipment may be of many forms and may be mounted in many different ways. For example, it may be packaged in a cabinet and mounted firmly to a floor or wall of the primary structure, or, alternatively, as in the case of complex systems with shock isolated platforms, it may, in turn, be mounted on these platforms. Attention is directed herein primarily to the former type of equipment, arrangement, and mounting. Typical of the types of equipment being considered are those described by such terms as switch gear, relays, circuit breakers, solid-state electronic devices, communication devices, optical equipment, sensors and control equipment, and heavy mechanical equipment (for example, pumps, piping, generators, heat exchanges, filters, and combinations thereof).

More often than not the equipment is mounted inside of a cabinet. Therefore, the first consideration with regard to evaluation for shock effects is the strength of the cabinet and the strengths of the mounting fixtures inside the cabinet. Generally this means that in addition to the components the cabinet itself needs to undergo testing and/or analysis as well as the mounting arrangements for components within the cabinet, and the supports for the cabinet. Shock tests have shown, in many cases, that an otherwise sound cabinet suffers a great deal of damage arising from insufficient cabinet bracing and

insufficient support arrangements for the equipment mounted in the cabinet.

In some cases, as for examples pumps, electric motors, and transformers, the item has feet or base support plates that in some cases may be cast metal or, alternatively, welded to the item. In some cases, these base mountings have proven to be weak links under shock conditions, especially if the metal is of a brittle nature.

Another design aspect in consideration of the equipment type is that of relative motion between pieces of equipment, or the equipment and a connector such as a pipe or cable bundle that goes to some other location. The connector may be subjected to relative deformation in such a way as to render it functionally disabled, and may impart distorting forces on the cabinet. Most testing machines are unable to simulate this type of behavior, although recently developed multiple exciter sources mounted over a test floor can replicate such behavior; for some systems, as for example piping, this topic needs special consideration in the design process.

One of the major concerns in assembling an equipment cabinet made up of components of various types from various manufactures is the fact that, even though each of the components individually may have been subjected to some particular test or analysis regime in terms of qualification, when mounted together as a system in a cabinet, the environment to which the equipment system may be subjected, in many cases, is quite different from that which the manufacturer may have envisioned. For that reason, in making up an assembled equipment item, it is important that those supplying the various components, as well as those designing the final assembled package, consider carefully the requirements for each individual item and then the requirements for the total package. Such design involves consideration of interactions, subsystem resonance, repeated motion, various forms of reversal of motion, possible racking of (striking) elements within the assemblage, etc.

Of equal importance to all the above, of course, is the mounting arrangement for the cabinet or item itself. This topic is treated separately in Section 2.5.

2.4 DESIGN ENVIRONMENTS OR "LOADINGS".

The design of a piece of equipment to resist ground shock motion for military systems is an extremely complicated and complex process. Many designers and criteria developers have the impression that the problem is one of merely defining the shock base motions and, thereafter, carrying out analyses or tests as desired to verify the adequacy of the design. In reality the design process is much more complicated and, if properly carried out, consists of consideration of an extremely large number of variables, each of which must be defined appropriately and in a form that can be used by the engineer or scientist in carrying out the total system design.

The design of the item, which might consist of a cabinet with numerous internal components, must be made first for the usual deadload considerations, in light of the manner in which the unit is mounted, and for the other normal loadings that would be expected under service conditions. These latter loadings may include vibration from live loads, normal and high winds if the item is exposed, seismic excitation, thermal effects, and the like. However, there are a host of other items that must be considered in the design and these are listed next.

With regard to the matter of the shock loading, perhaps intense shock type loading that may arise as a result of a nuclear detonation nearby, the following factors normally would need to be considered and defined in detail as a part of the design criteria, and employed appropriately as part of the overall design process.

1. Overpressure and dynamic pressure effects, including reflections
2. Ground shock effects
   a) Translation type motions transmitted to the base attachment zone in the form of acceleration, velocity, and displacement, as a function of time, or alternatively, representation in other input forms such as possibly spectra
   b) Rotational type motions, if appropriate

c) Relative motions between support points, and at attachment points for piping, cables, etc.

d) Impulse and momentums transfer as they may affect the equipment, including "trapped" impulse

3. Thermal shock of various forms
4. Radiation of various forms
5. Electromagnetic effects
6. Impact by ejecta
7. Accoustical noise effects
8. Reversal of motions and/or rebound effects
9. Multiple loadings from several blasts

Other factors typically that might be expected to be a consideration in the design "loading" environment are the following:

1. Effects of humidity
2. Sand and dust
3. Fungus and bacterial growths
4. Fire and toxic gases
5. Sustained vibration arising from transportation of the equipment to the site, or from excitation caused from nearby machinery
6. Impact arising from racking should the equipment strike any nearby objects
7. Corrosion
8. High explosive effects such as those associated with conventional weapons or terrorist activities
9. Medium to high frequency vibration (mechanical) environments
10. Role of "aging" with time under use or stand-by conditions, including considerations of maintenance over the years.

Item 10 is often overlooked; the functionability of the equipment at various stages in its life needs careful consideration, i.e., will the functionability be the same after it has been in service for several years and, if subjected to shock at that time in an aged

condition, can the performance be expected to be the same as that when it was somewhat newer?

It should be obvious from this listing that a great deal of effort will have to be expended in developing the environmental information or loading criteria that will be needed for the design process. These criteria must be thoroughly thought out on an individual basis with regard to the reasonable limits that can be expected during the service life, during attack, and considerations given to what happens if the intensity of the environment is somewhat greater even than the design level. For example, will any one factor, or any combination compromise the functioning of the system.

Also, what effect will loss of the item have on overall system performance?

As a part of these considerations, one must give careful attention to what combinations of these environments are important and how can they interact with each other in leading to critical loading conditions. Often combinations of "loadings" at other than peak values can lead to control of certain phases of the design. This aspect of the design process is one of the most important if a satisfactory design is to be achieved.

2.5 EQUIPMENT RESISTANCE AND EQUIPMENT MOUNTING.

2.5.1 Equipment Resistance.

From a gross viewpoint, the equipment item as a whole as well as the internal components, must be able to withstand the anticipated design loadings of the type outlined in Section 2.4. It is this aspect of design qualification to which the procedures presented in Ref. 13 are directed. However, piecemeal application of such procedures to components or assembled units does not necessarily insure satisfactory system performance.

For most complex equipment assemblies the design process is actually quite complicated, involving many individuals, each concerned about different aspects of the equipment item. The chief engineer, or director of manufacturing, must insure that the design criteria are met in all respects and be ready to comment when such criteria may appear

inappropriate. Design and manufacturing communication, often nonexistent, should be encouraged. But even moreso, the assessment of adequacy must include some measure of the margin of safety, or more succinctly the margin of overloading (based on consideration of all applicable environmental loadings) to achieve a state of damage that would render the equipment unfunctionable. Unfortunately in recent years, physical vulnerability analyses have revealed that these limits and margins were not well defined in many cases.

For example, one sensitive item often found in equipment shock testing is that of wire leads (often bundles) running between pieces of electronic equipment, or to a connector board. In many cases, these leads can be subjected to significant force and/or deformation, or are fatigue sensitive; in such cases, these connector leads can turn out to be the weak point in the system performance.

In other cases the limiting damage states may center around yielded shafts, distorted bearings, broken welds, sheared bolts, ruptured hydraulic lines to sensors and gages, distorted display gates, etc., any one of which could render the equipment incapable of functioning properly.

Over the years the most common descriptor employed for describing equipment damage is acceleration. The reasons for this choice of description are many, including the facts that the most commonly used instrument for measurements is the accelerometer, that acceleration is in some measure a descriptor of force, and that it is a single simple parameter. For many cases, especially those where significant deformation occurs, velocity probably would be a better and more stable indicator and, to some degree, reflects the energy state. As a result of research and observations it has become increasingly apparent that acceleration alone is not a particularly good indicator, especially for moderate to highly ductile systems; for example, seismic fragility studies have shown that high spikes of high frequency motion usually have little damaging effect in much the same way as high frequency high acceleration level excitation is not particularly damaging to well designed equipment in other application environments.

Thus, through careful design, with appropriate analysis and testing as required, the designer conceptually assembles the item, at all times keeping in mind the functional goals, the loading environments, and the role of the item in the system. If the equipment item is quite critical, the system designers quite likely will provide backup systems of a redundant nature, if possible.

2.5.2 Equipment Mounting.

The subject of mounting of the equipment is of such great importance that it is singled out for special discussion in almost every report or book written on the subject of shock problems. The reason for this attention is the fact that the mounting, in essence, serves as the resisting element or support element between the equipment item and the primary structure on which the equipment is mounted. This, in turn, means that the properties and the behavior of this mounting element must be fully understood if there is to be a good design for which the response of the equipment item is to be evaluated in a rational manner. Similarly, of course, the individual internal items of equipment inside of the gross equipment item, as for example a cabinet, must be examined in the same manner in the sense of how they are mounted so as to insure that their functionability will not be impaired under the various "loading" environments, singly or in combination, including shock loadings. Experience has shown that careful attention to mounting will, in many cases, serve to preclude shock damage.

For purposes of analysis, and for purposes of design and construction of the equipment mounting, it is necessary to have an understanding quite early in the process as to whether or not it is desired to maintain the mounting element in a linear condition, permit it to go nonlinear and in what form (elastoplastic, or elastic hardening, or strain softening), or to transit the energy on into the equipment where it will be absorbed. More specifically, it is necessary to ascertain the nature of the energy absorption that is desired anywhere the energy is to be absorbed. For example, is the energy to be absorbed by the supports in one or more of the three

translational directions, or in one of the complex internal modes of response of the equipment including possibly rotational modes? Also, the designer must be concerned with the possibility of repeated loadings, as well as loadings that lead to motions of both a positive and negative type. More than the foregoing, the support devices should be able to handle the maximum design shock-type loadings defined in the criteria, although the definition of maximum in this case may consist of a combination of environments. However, in addition, the supports should be able to handle other variations of loading, as for example, high frequency excitations at perhaps somewhat lower or higher levels than the maximum design levels, and various combinations thereof. This factor is often overlooked in shock design of equipment, namely that the loadings of concern in the design process may not be solely those associated with "the maximum" of some of the environments considered; a combination of some of the environments at a slightly lower level may lead to an even more severe condition. And, last but not least, to repeat, the designer must fully understand the response or behavior anticipated to be reasonably assured of adequate performance of the supports as well as the equipment itself. Only in this way can the design lead to reasonable performance of the mountings and equipment under the loadings.

The matter of the materials used in the mountings is of paramount importance, particularly with regard to their properties when subjected to these severe environments. Normally one thinks, first of all, about the strength of the materials, their ductility (ability to undergo large deformation and to absorb energy, monotonically or under repeated reversals), their ability to be machined, pressed, forged or joined (bolting, welding, and gluing of various types) all of which can affect the performance of the mounting or equipment item. Additional considerations may exist with regard to provision of bumpers or snubbers should the motions go beyond some specified limit.

Another consideration is that of ascertaining the nature of isolation that might be provided by certain types of connectors. This topic of shock isolation has been the subject of numerous research papers and reports and is treated in many books (Refs. 14 through 16);

for certain applications, this technique is clearly the mode of support that should be employed. On the other hand, under many severe environments where there is uncertainty as to the range of the frequencies and the amplitudes of the excitation that may occur, it is quite possible that no one single support isolator system is adequate. In such cases, one must be concerned about the transmission of motions through the isolators, the bottoming out of the isolators, and the motions transmitted to the equipment under these conditions.

Quite obviously then the same types of considerations must be given to the components that make up the equipment item. For example, if the cabinet contains lots of interior items that are individually mounted, each of these in turn must receive the design attention just described. In addition, interaction effects between the various components needs careful consideration.

A sketch depicting a typical piece of equipment and one mounting strategy is shown in Fig. 16.

2.6 CHARACTERIZATION OF SHOCK MOTIONS.

It is difficult to find any one definition of shock motion that is all encompassing, but in Chapter 1 of Ref. 14, the definition is given for mechanical shock as follows. "Mechanical shock is a nonperiodic excitation (e.g., a motion of the foundation or an applied force) of a mechanical system that is characterized by suddenness and severity, and usually causes significant relative displacements in the system." A second good and related definition is given in Chapter 44 on page 2 of Ref. 14, wherein the following is stated. "...A shock wave is a discontinuous pressure change propagated through a medium at velocity greater than that of sound in the medium. In general, forces reaching peak values in less than a few tenths of a second and of not more than a few seconds duration may be considered as shock forces in relation to ...". Actually the velocity criterion noted may or may not be entirely representative of all shock situations.

Both of the foregoing definitions clearly imply a transient type motion which may be either short or rather long in duration and may have many changes in signal in the intervening time period. In this

sense then, it is quite common to specify the shock motions in such forms as functions solely of peak acceleration, peak velocity or peak displacement, or alternatively as functions of amplitude (acceleration, velocity or displacement) and time, in each of the directions under consideration. Typical examples of shock motions of this type are shown in Fig. 17.

Alternatively, displacement versus time might be defined for some types of applications. It is difficult, if not almost impossible, to arrive at prescribed forms of acceleration and velocity, however, through a displacement-time prescription.

It suffices to say that a good definition of the shock motions requires detailed knowledge of the nature of the expected shock excitation and involves some very careful detailed input as to the nature of the motions. Attention should be given to the consistency of the defined motions in the sense that the maximum velocity should be associated with the time when the acceleration passes through zero and, likewise, the maximum deformation should be associated with the time when the velocity passes through zero. Obviously there can be a residual deformation at late times. If the motions are defined at very early times and very late times, the controlling bounds in such case would be that the acceleration would be zero if one went to an early enough time and a late enough time; likewise for velocity the bounds would be the same. For displacement, at an early time the value should be zero; the final displacement at a late time need not be zero, but clearly could have a residual. These "controls" are discussed in certain signal processing texts, and in a few texts on structural dynamics.

Another form of characterization of the shock motions is that of the response spectrum or shock spectrum. Basically the response or shock spectrum is defined as the peak response (normally acceleration, velocity, or displacement) of a single-degree-of-freedom (SDOF) oscillator plotted as a function of frequency. The SDOF oscillator may be depicted as shown in Fig. 18 for the case of base excitation; in this figure the y-terms denote the base excitation motions, the x-terms the motions of the mass, and the z-terms denote the relative motions.

The theory behind response or shock spectra is not presented here; instead the reader is referred to Chapter 29 of Ref. 15 for an elementary discussion of spectra, and to other chapters in the same reference for related discussions. Generally the base excitation values (y-terms) may be known or given. Of particular interest from an engineering standpoint, normally, are the following: (a) the acceleration of the mass since it provides some indication of the force in the spring; (b) the relative deformation of the spring in as much as it provides a measure of the deformation of the spring; and, (c) the relative velocity as it provides some measure of the energy imparted into the system.

The subtle point is made here with respect to a response spectrum (based on analysis of an S-D-O-F system) for a given excitation, and a design spectrum which consists of a specified (desired) characterization as may be needed for design. Depending on its origin or use, a shock spectrum could fall into either of the above categories.

The spectra plots can be made in many ways. For example, the velocity, as a function of frequency, might be plotted as shown in Fig. 19(a). In this plot the "true velocity", or $\dot{u}$, is indicated thereon, and differs from the pseudo-velocity (defined as ωu) in the low and high frequency regions. In the central region, for modest forms of excitation such as those associated with earthquakes and high explosive blast, the two values are essentially the same. For very high frequency motions the spectra are more difficult to define in a manner that is of general engineering design usefulness; this topic of high frequency response deserves special study, especially in the case of intense shock excitation.

An even more revealing technique for plotting shock spectra can be obtained through the use of so-called tripartite plots, wherein acceleration, velocity, and displacement are plotted as a function of frequency on one sheet (Fig. 19(b)). The details of this type of plot are not discussed here except to note that studies in depth, especially for earthquake motions in recent years, have shown the dependency of the expected bounds, and the width of the response spectrum, to be

items which can be calculated or estimated with reasonable accuracy depending upon the nature of the conditions that are known about the excitation, (Ref. 15).

Shock spectra are sometimes obtained in an entirely different way, namely, one can mount an instrument on the ground or on a piece of equipment and, through measurements of the response of the system, obtain some of the peak transient response values directly. One good example is a reed gauge, which consists of a number of single-degree-of-freedom oscillators mounted inside of a box-like container. When the box is excited, values of peak displacement are recorded which, in turn, can be interpreted and plotted as a function of frequency. In turn, these points define the spectrum. It is in this manner, in fact, through devices of this type, that checks on both the calculation and measurements of response spectra have been obtained in practice.

For items of equipment mounted in turn on responding elements in the structure, significant additional amplification is possible. For example, an equipment item mounted on a wall would be expected to experience essentially the same excitation as the wall. On the other hand, if the item is mounted on a floor the input will reflect the motion of the floor. For modest excitation, such as that associated with earthquakes, these observations have led to plots called "floor response spectra" (FRS), and the motions associated with light equipment mounted on upper levels of a facility, for example, can be many times the base excitation. The dotted "bump" in Fig. 19(b) depicts such amplified motion. Of course, as the supported equipment becomes heavier, significant interaction between the equipment item and the base structure can occur. This matter of interaction, especially for large base excitation such as occurs in a missile silo, and the need to reduce the motion imparted to suspended objects, is the reason for employment of shock isolation systems.

Moreover, as discussed in Ref. 15, it is possible for modest amounts of deformation for one to make estimates of modified response spectra to reflect the effects of nonlinear motion. Nonetheless, these modified response spectra, sometimes called "inelastic response

spectra", have been developed in a rather simple and approximate manner to reflect the effects of inelastic behavior and the energy absorption that takes place with the amelioration of the motion. The development of modified spectra are based primarily on monotonic type resistance considerations. For transient loading with cyclic response and significant nonlinear behavior, research is just beginning to point the way for handling such situations in a design environment as discussed briefly below.

Within the last several years, those individuals closely associated with the background and use of the response spectrum have come to realize some of the shortcomings of the response spectrum for use in design; this observation includes especially the use of the modified response spectrum. As a plot of peak value versus frequency, a response spectrum does not reflect well the aspects of behavior associated with yielding and hysteretic behavior, especially under motions that lead to positive and negative response. Damping, when it can be modelled by Coulomb damping (time-dependent velocity damping) can be handled through use of the response spectrum reasonably well. For more complex types of damping, as for example frictional damping, especially where the friction may act intermittently, no good techniques for handling such behavior through use of response spectra exist. Other recent studies have centered on frequency content versus peak response and as a result some design criteria now call for a check of power spectral density. On the other hand, it turns out that there is nothing generally unique about the response spectrum in that there are a large number of different motion time histories can lead to a response spectrum which satisfactorily bounds a characteristic smoothed design spectrum. In this connection, special attention needs to be given to synthetic time-history base motions to ensure that the response characteristics are indeed those applicable to design.

The situation is even more complex when one realizes that there can be phasing problems, perhaps differential phasing of the excitation that are fed into the multiple mounts of an equipment item, and the situation becomes even more complex when one must take into consideration both translation and rotation which is usually the case.

For these reasons, although the response spectrum is useful for characterization and for simple input for some forms of calculation, in most complex ground supported equipment systems it would be expected that of greatest importance would be the expected (or specified) translational or rotational time-history functions of the motions at the supports which could be used in numerical computation. This form of input is especially desired for cases wherein detailed study of the nonlinear response is desired or where input phasing studies are to be carried out.

2.7 ANALYSIS TECHNIQUES.

An excellent discussion of the analysis techniques commonly employed for systems subjected to shock is contained in Chapter 42 of the Shock and Vibration Handbook, (Ref. 15). As pointed out there, the first important aspect of the analysis procedure is to examine the modelling of the system to be sure that the important components are correctly modelled with regard to their mass, support characteristics (resistance properties), damping, and other factors which enter into the behavior of the elements and in their subsequent response. The definition of the item to be studied is not a simple matter, and one that is deserving of much more study than is commonly given to the subject. In fact, it is advisable to carry out a rather well thought out parameter variation analysis if the equipment item is to be analyzed in a form in which the response characteristics are to be believed with any degree of assurance. Clearly the more complex the model, the more difficult the analysis, and most likely the more difficult the interpretation of the results. The most is known about single-degree-of-freedom systems, a lesser amount about two-degree-of-freedom systems, and even less about the handling of multi-degree-of-freedom systems. In some cases, these latter systems can be handled through standard modal analysis procedures including the use principal modes and, thereafter, the combination of modal responses, but in many cases this is not possible especially where the system has coupled modes and where the response is nonlinear.

Shock response calculations can be very expensive and time consuming and should be carefully thought through before work is started. A systematic and carefully structured pilot-type scheme for calculation, especially where a rational set of parameter variations is included, usually leads to a reasonable overview of possible response. The parameters normally calculated include such factors as displacement, velocity, acceleration, rotation, absorbed energy, etc. A well planned modelling and calculational approach permits one to go back and recycle through the process and subsequently arrive at a satisfactory design, or judgments as to what would constitute a satisfactory design, or analysis, as the case may be.

An entirely different approach can be employed based on probabilistic considerations. This approach becomes more complex in the sense that one is looking statistically at a variation of parameters and must make a number of judgments as to the importance of these parameters as they are combined to arrive at the design in terms of exceedance limits and related matters. The recent studies in connection with nuclear power facilities and equipment (Probabilistic Risk Assessment [PRA] studies) has given new insight into this approach for assessing existing facilities. In this connection, Fig. 20 (taken from Ref. 17) is provided to indicate one approach to this scheme of analysis that might be worthy of further investigation with regard to shock excitation and assessment.

2.8 SHOCK TESTING.

A rather comprehensive discussion of shock testing machines and techniques for carrying out shock testing are presented in numerous references; one good treatment is that presented in Chapter 26 of the Shock and Vibration Handbook (Ref. 15).

There are a great many types of shock testing machines located in laboratories throughout the United States. As the descriptive material in Chapter 26 of Ref. 15 indicates, such machines are generally classified by the type of shock that is input through the testing table. Designations such as "velocity" or "step velocity change", "simple half-sine acceleration shock pulse", "rectangular force pulse",

"single complex shock", and "multiple shock pulse" are typical of those commonly assigned to shock test devices. As one might surmise, the physical nature of the tables varies greatly, and the nature of the shock pulse is determined by the manner in which the pulse is generated. For example, electromagnetic tables or electrohydraulic ram excitation type tables can provide systematic and reliable excitation for low levels and even moderate levels of transient excitation. However, higher levels of shock testing up to this time normally involves a different kind of machine, as for example those achieved by drop tests, in which the equipment is mounted on a table that falls and is deaccelerated by a special device. In some cases, these tables follow inclined surfaces and include the effects of various kinds of springs and dashpots. In other uses air guns or pendulums are used for impacting objects; in some cases, objects are mounted on high speed sleds that are deaccelerated rapidly.

It should be obvious that one of the principal problems in the shock testing field is that of selecting or specifying the shock test conditions that are characteristic of the design situation, and that will lead to evaluation of design adequacy in a meaningful manner. Preferably, in many cases, a range of shock inputs to be employed in testing are desired.

Another technique often employed for shock testing is that of testing with high explosive or nuclear detonation sources. This type of testing is quite expensive and time consuming, but for certain types of situations is almost a necessity if large-scale or near full-scale response results are to be obtained. One cannot help but believe, in view of the costs involved, that more "piggybacking" of various test programs should be undertaken to acquire more vulnerability, fragility and margin type information.

In light of the previous discussion of loading environments and combinations thereof, one can readily observe that the testing processes, which are very important in qualification of equipment, have limitations on what can be achieved. For this reason, the ability to analyze the items is becoming of increasing importance. However, in making this observation, it is important to note that shock tests, in

many cases, show up deficiencies that would almost never be discovered through analysis. For this reason, it is normally wise and prudent to have shock tests of some sort carried out on equipment to ascertain that, at least to some degree, the severe environments represented by the testing process can, indeed, be met by the equipment item. Also, it is only rarely for the very intense shock environments that actual testing experience can provide data points for cross checking against the analysis predictions.

2.9 GENERAL OBSERVATIONS PERTAINING TO DESIGN.

This short treatment on the design of equipment to resist ground shock hopefully should serve as an overview for someone who wishes to design, or analyze from a vulnerability point of view, ground supported equipment that is excited by the ground motions arising from a weapon blast or other sources of excitation. It should be obvious from the presentation that, in developing the criteria and studying the environment, a great deal of work is required in properly defining the environments in a form that can be used in a design/analysis process, both in terms of analysis of a representative system or subsystems, as the case may be, and/or used in specifying testing approaches in examining the response of the system and its adequacies or shortcomings. And, it should be noted again that such considerations should be given, not only to the equipment in its new design state, but also should reflect all of those properties that might be required down the line after the equipment has been in operation for some extended period of time, i.e., after it has aged some. A major question at that time is will it function in a manner that is appropriate and in line with the original design objectives?

At some stage clearly there must be an assessment in some form of the possible damage levels as discussed briefly earlier herein. In many cases, current shock design and testing criteria employ assessment schemes that are based solely on acceleration. Often acceleration is not found to be a very descriptive damage indicator, and, in fact, if energy input is believed to be of importance it is intuitively obvious that velocity should be a more descriptive indicator. Moreover, high

spikes of acceleration do not necessarily lead to significant damage, especially if associated with high frequency motions. In some cases distortions or displacements are the indicative measures of importance. At present there is no clear set of measures that can be cited as damage indicative, and, in fact, this aspect of the design criteria is one of the most difficult topics to address. A great deal more work in this area is needed. As one example of the methods employed in the past to depict damage, and, in turn, to arrive at damage response levels, Fig. 21 is presented. In this figure the damage ranges in terms of frequencies and acceleration levels is shown, and as the shock levels are increased (a), (b), and (c), it will be noted that the shock spectrum curve intersects the damage zone. With recent advances in estimating response where nonlinear behavior is involved, and new understanding of response that is not depicted in shock spectra, it should be possible to arrive at even better ways of evaluating damage. This topic is one portion of the studies to be carried on in the next phase of this ongoing investigation.

Following the design of an equipment item, or as a part of the vulnerability analysis process, one is always looking for the weak link or "common denominator" that will lead to degradation of the equipment or that will compromise its functionability. In view of the large number of factors that must be considered in terms of the environments to which it may be subjected and the possibilities of various complex types of motions which this equipment may experience, the process becomes one of trying to be sure that all of the major important excitations and environments are indeed examined. It is not easy to be sure that this objective has been achieved and it is for this reason that there is increasing attention in recent years to the probabilistic approaches in this field to perhaps increase our confidence as to the effects of a variety of inputs and responses.

If one attempts to take existing articles and even handbooks, for example the Shock and Vibration Handbook, and assemble a logical process for handling the shock validation for a piece of equipment, it is easy to become confused and to lose the stream of logic that should be carried forward to arrive at a successful design and/or analysis

approach. It is hoped that this treatment will serve to provide a basic "roadmap" for the designer or analyst who is looking for guidance in this particular area.

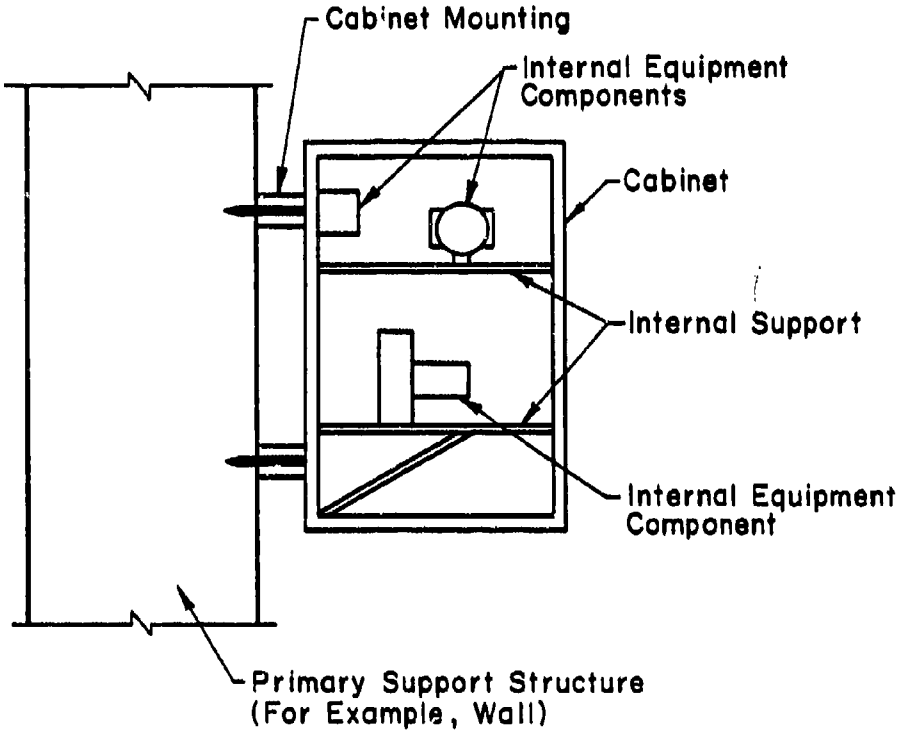

Figure 16. Schematic cross-section of mounted cabinet with internal equipment components.

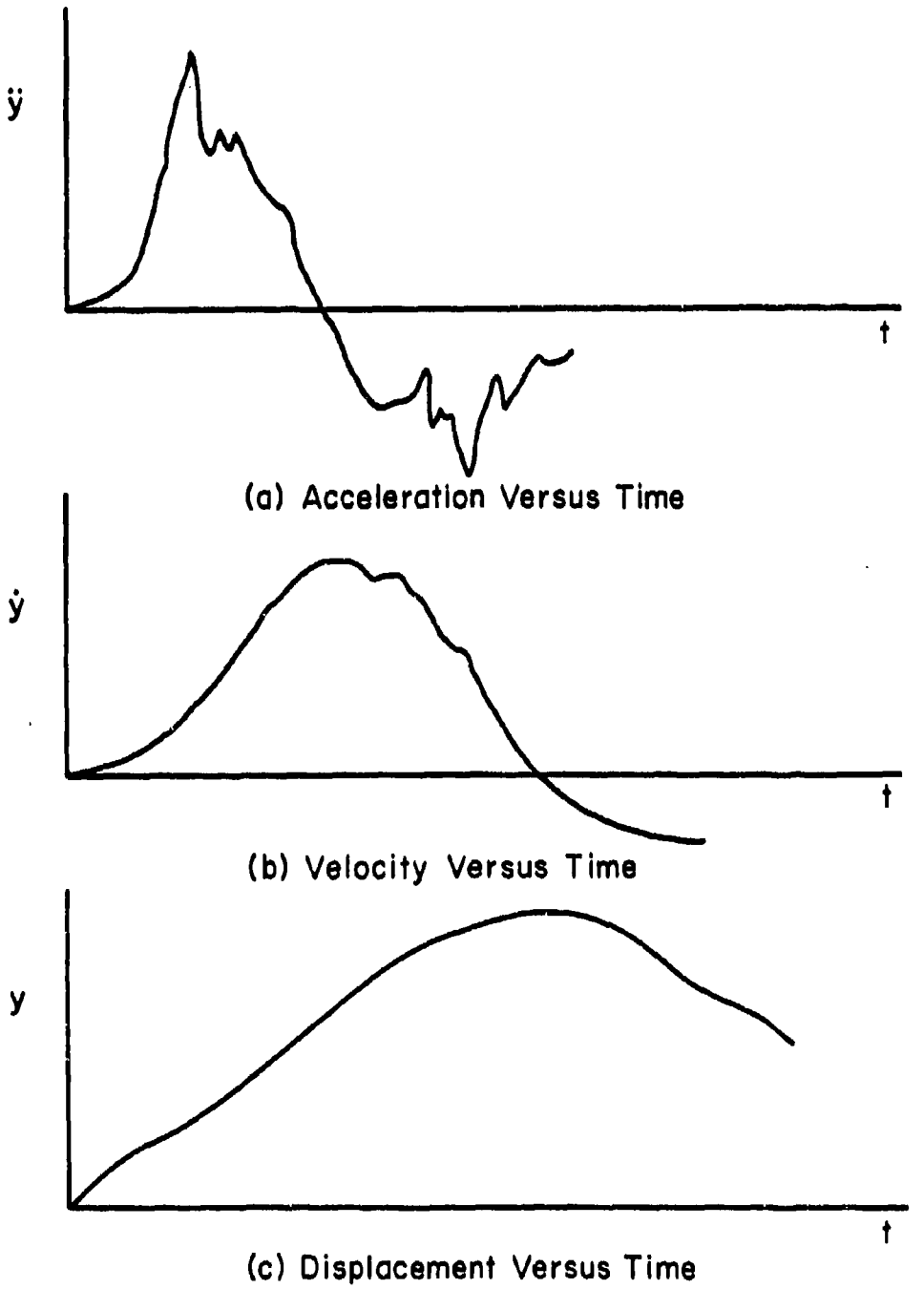

Figure 17. Typical ground shock motion.

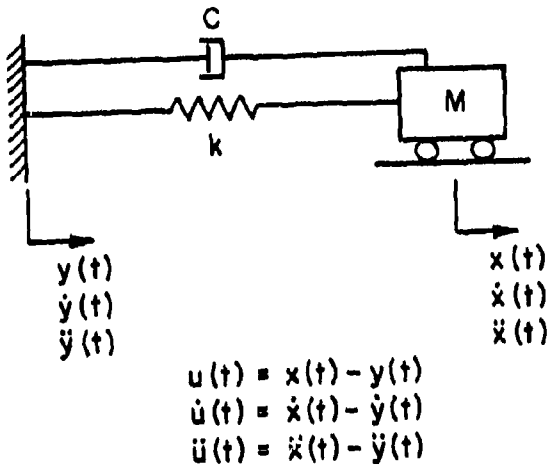

Figure 18. Single-degree-of-freedom linear oscillator.

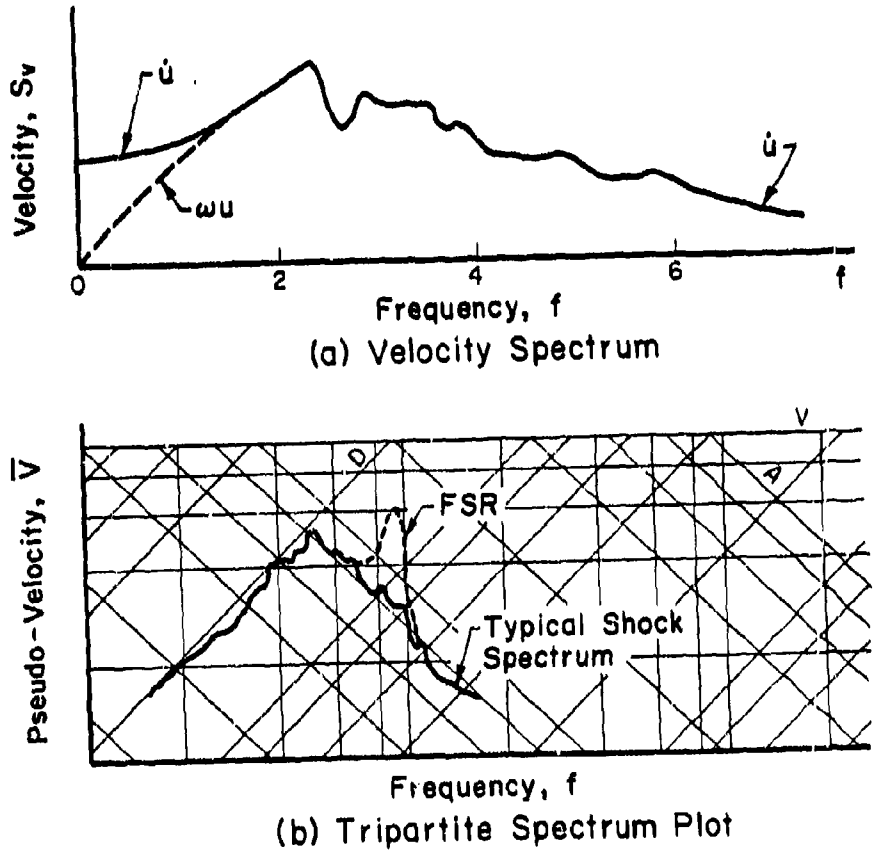

Figure 19. Examples of response or shock spectra.

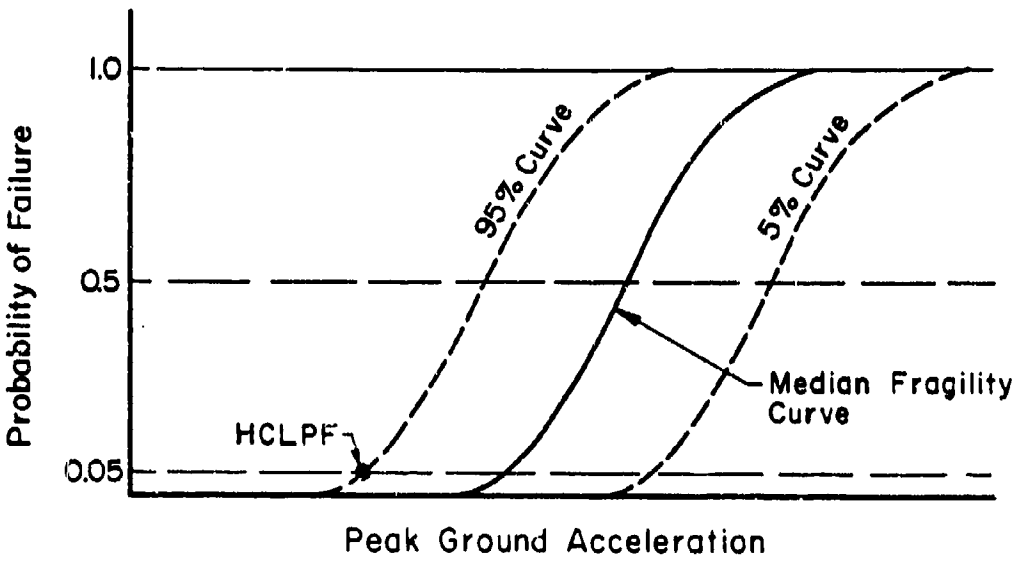

Figure 20. Schematic of high confidence low probability of failure (HCLPF) concept.

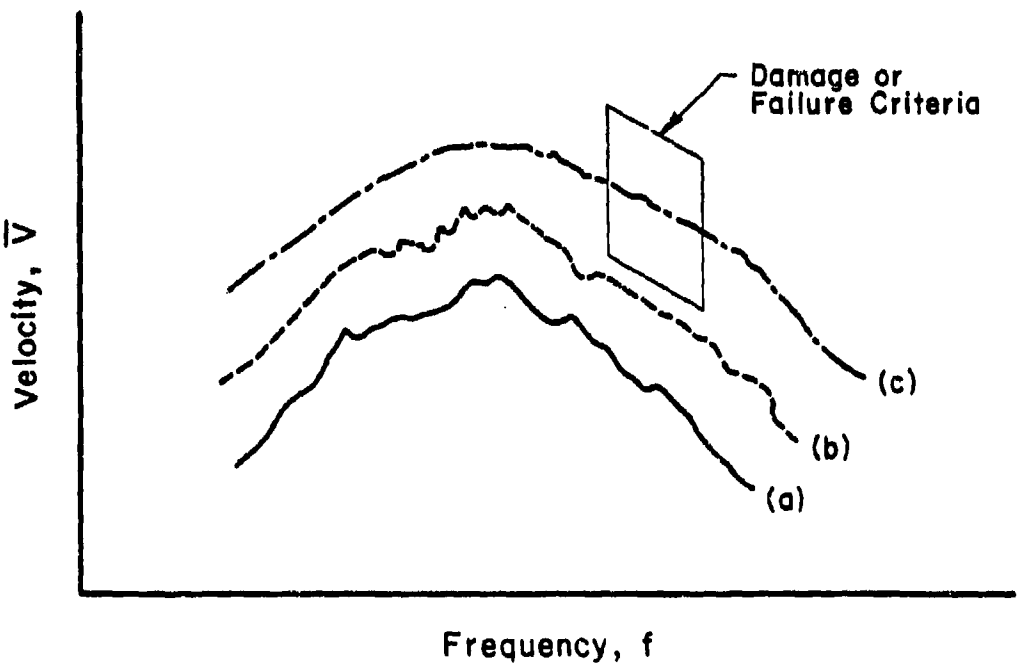

Figure 21. Response versus damage.

SECTION 3

LIST OF REFERENCES

1. Kiger, S. A. and J. V. Getchell, "Vulnerability of Shallow-Buried Flat-Roof Structures, Report NO. 1, Foam HEST 1 and 2", Technical Report SL-80-7, September 1980, U.S. Army Engineer Waterways Experiment Station, Vicksburg, Mississippi.
2. Getchell, J. V. and S. A. Kiger, "Vulnerability of Shallow-Buried Flat-Roof Structures, Report NO. 2, Foam HEST 4", Technical Report SL-80-7, October 1980, U.S. Army Engineer Waterways Experiment Station, Vicksburg, Mississippi.
3. Getchell, J. V. and S. A. Kiger, "Vulnerability of Shallow-Buried Flat-Roof Structures, Report NO. 3, Foam HEST 5", Technical Report SL-80-7, February 1981, U.S. Army Engineer Waterways Experiment Station, Vicksburg, Mississippi.
4. Getchell, J. V. and S. A. Kiger, "Vulnerability of Shallow-Buried Flat-Roof Structures, Report NO. 4, Foam HEST 3 and 6", Technical Report SL-80-7, December 1981, U.S. Army Engineer Waterways Experiment Station, Vicksburg, Mississippi.
5. Kiger, S. A. and J. V. Getchell, "Vulnerability of Shallow-Buried Flat-Roof Structures, Report NO. 5, Foam HEST 7", Technical Report SL-80-7, February 1982, U.S. Army Engineer Waterways Experiment Station, Vicksburg, Mississippi.
6. Slawson, T. R., "Dynamic Shear Failure of Shallow-Buried Flat-Roof Reinforced Concrete Structures Subjected to Blast Loading", Technical Report SL-84-7, April 1984, U.S. Army Engineer Waterways Experiment Station, Vicksburg, Mississippi.
7. Kiger, S. A., T. R. Slawson, and D. W. Hyde, "Vulnerability of Shallow-Buried Flat-Roof Structures, Report NO. 6, Final Report: A Computational Procedure", Technical Report SL-80-7, September 1984, U.S. Army Engineer Waterways Experiment Station, Vicksburg, Mississippi.
8. Dallriva, F. D. and S. A. Kiger, "Data Report for FY85 1/2 Scale Box Structure Test", January 1985, U.S. Army Engineer Waterways Experiment Station, Vicksburg, Mississippi.
9. "Data Report for the Shallow-Buried Structures Height-of-Burst Test Series", March 1985, U.S. Army Engineer Waterways Experiment Station, Vicksburg, Mississippi.

10. Newmark, N. M., "A Method of Computation for Structural Dynamics", Journal of the Engineering Mechanics Division, ASCE, Vol. 127, 1962.

11. "Some Observations on Vulnerability Assessment Procedures For Buried Structures and Equipment (Part A - Influence of Resistance Function Uncertainties on Damage Radii For Shallow-Buried, Flat-Roofed Structures, by J. D. Haltiwanger; and, Part B - Observations on Ground Shock Resistance of Structures and Equipment, by W. J. Hall)", Final Report For Period 06/20/81 - 07/20/82, for Defense Nuclear Agency, contract DNA 001-81-C-0200, J. D. Haltiwanger Consulting Engineering Services, 20 July 1982, 71p.

12. "Some Observation on Vulnerability Assessment Procedures for Above-Ground Structures and Equipment" (Part A - An Exploratory Study of the Effects of Height-of-Burst on the Sensitivity of Damage Pressure Levels to Weapon Yield for Selected Typical Structures, by J. D. Haltiwanger; and Part B - Theoretical Observations on Ground Shock Resistance of Simple Structures and Equipment - Part II, by W. J. Hall and S. L. McCabe), Final Report for Period 10/12/82 - 12/12/83, For Defense Nuclear Agency, Contract No. DNA001-83-C-0067, J. D. Haltiwanger Consulting Services, 30 December 1983 (Revised 15 May 1984).

13. "Military Standard -- Environmental Test Methods", MIL-STD-810C, 10 March 1975.

14. Shock and Vibration Handbook, 1st Edition, edited by C. M. Harris and C. E. Crede, McGraw-Hill Book Co., 1961.

15. Shock and Vibration Handbook, 2nd Edition, edited by C. M. Harris and C. E. Crede, McGraw-Hill Book Co., 1976.

16. Crede, C. E., Shock and Vibration Concepts in Engineering Design, Prentice-Hall, Inc., 1965.

17. Budnitz, R. J., P. J. Amico, C. A. Cornell, W. J. Hall, R. P. Kennedy, J. W. Reed, and M. Shinozuka, An Approach to the Quantification of Seismic Margins in Nuclear Power Plants, Lawrence Livermore National Laboratory, NUREG/CR-4334 UCID-20444, prepared for U. S. Nuclear Regulatory Commission, July 1985.

DISTRIBUTION LIST

DEPARTMENT OF DEFENSE

DEFENSE INTELLIGENCE AGENCY
ATTN: DB-4C RSCH PHYS VULN BR
ATTN: DB-6E2, C WIEHLE
ATTN: RTS-2B
ATTN: S HALPERSON

DEFENSE NUCLEAR AGENCY
ATTN: STSP
4 CYS ATTN: STTI-CA

DEFENSE TECHNICAL INFORMATION CENTER
12 CYS ATTN: DD

DNA PACOM LIAISON OFFICE
ATTN: J BARTLETT

FIELD COMMAND DEFENSE NUCLEAR AGENCY
ATTN: FCTT W SUMMA

JOINT CHIEFS OF STAFF
ATTN: J-5 NUC & CHEM DIV

JOINT STRAT TGT PLANNING STAFF
ATTN: JLK (ATTN: DNA REP)

DEPARTMENT OF THE ARMY

U S ARMY COLD REGION RES ENGR LAB
ATTN: LIBRARY

U S ARMY CONSTRUCTION ENGRG RES LAB
ATTN: LIBRARY

U S ARMY ENGINEER CTR & FT BELVOIR
ATTN: TECHNICAL LIBRARY

U S ARMY ENGR WATERWAYS EXPER STATION
ATTN: J BALSARA, WESSS
ATTN: S KIEGER, WESS
ATTN: TECHNICAL LIBRARY

DEPARTMENT OF THE NAVY

CARDEROCK LABORATORY
ATTN: LIBRARY

NAVAL POSTGRADUATE SCHOOL
ATTN: CODE 1424 LIBRARY

DEPARTMENT OF THE AIR FORCE

AIR FORCE INSTITUTE OF TECHNOLOGY
ATTN: LIBRARY/AFIT L DEE

AIR FORCE WEAPONS LABORATORY, AFSC
ATTN: NTE M PLAMONDON
ATTN: NTED R HENNY

BALLISTIC MISSILE OFFICE/DAA
ATTN: MYED D GAGE

FOREIGN TECHNOLOGY DIVISION, AFSC
ATTN: NIIS LIBRARY
ATTN: S SPRING

DEPARTMENT OF ENERGY

UNIVERSITY OF CALIFORNIA
LAWRENCE LIVERMORE NATIONAL LAB
ATTN: L-53 TECH INFO DEPT LIB

DEPARTMENT OF DEFENSE CONTRACTORS

ACUREX CORP
ATTN: C WOLF

AGBABIAN ASSOCIATES, INC
ATTN: M AGBABIAN

APPLIED RESEARCH ASSOCIATES, INC
ATTN: N HIGGINS

APPLIED RESEARCH ASSOCIATES, INC
ATTN: S BLOUIN

APPLIED RESEARCH ASSOCIATES, INC
ATTN: D PIEPENBURG

BOEING CO
ATTN: M/S 13-13 S STRACK

BOEING TECHNICAL & MANAGEMENT SVCS, INC
ATTN: AEROSPACE LIBRARY
ATTN: M/S 13-13 S STRACK

CALIFORNIA RESEARCH & TECHNOLOGY, INC
ATTN: LIBRARY

CALIFORNIA RESEARCH & TECHNOLOGY, INC
ATTN: TECH LIB

GIBBS & COX
ATTN: R KHONDKER

H & H CONSULTANTS, INC
ATTN: E CORDING
2 CYS ATTN: J HALTIWANGER
2 CYS ATTN: W HALL

DEPT OF DEFENSE CONTRACTORS (CONTINUED)

KAMAN SCIENCES CORP
ATTN: D SEITZ

KAMAN TEMPO
ATTN: DASIAC

KAMAN TEMPO
ATTN: DASIAC

KARAGOZIAN AND CASE
ATTN: J KARAGOZIAN

MARTIN MARIETTA CORP
ATTN: K PAYNE

MERRITT CASES, INC
ATTN: LIBRARY

PACIFIC-SIERRA RESEARCH CORP
ATTN: H BRODE, CHAIRMAN SAGE

R & D ASSOCIATES
ATTN: J LEWIS

R & D ASSOCIATES
ATTN: J WEBSTER

TRW ELECTRONICS & DEFENSE SECTOR
ATTN: R CRAMOND

WEIDLINGER ASSOC, CONSULTING ENGRG
ATTN: T DEEVY

WEIDLINGER ASSOC, CONSULTING ENGRG
ATTN: M BARON

WEIDLINGER ASSOC, CONSULTING ENGRG
ATTN: J ISENBERG